IMPACT PRESSURE AND TOTAL TEMPERATURE INTERPRETATION AT HYPERSONIC MACH NUMBER

Thesis by

Jack C. Graves

Lieutenant, U. S. Navy

In Partial Fulfillment of the Requirements

For the Degree of

Aeronautical Engineer

California Institute of Technology

Pasadena, California

1954

ACKNOWLEDGMENTS

The writer wishes to express his appreciation to Dr. H. T. Nagamatsu for his support and guidance throughout this investigation. Sincere thanks are extended to the staff of the GALCIT Hypersonic Wind Tunnel for their complete cooperation, to the members of the GALCIT Machine Shop who skilfully fabricated the test equipment, and finally, to Mrs. H. Van Gieson, Miss Fae Scheinis, and Miss Natalie Waldron for their aid in the preparation of the final manuscript.

ABSTRACT

Results are presented of an experimental investigation of impact-pressure and total-temperature interpretation at a nominal Mach number of 5.6. The data indicate that the Rayleigh equation, which assumes non-viscous flow, requires correction at low free-stream Reynolds numbers. These viscous effects are detected at Reynolds numbers (based on impact-probe diameter) as high as 6000, and they continue to increase with decreasing Reynolds numbers. At the low pressure limit of the facilities used in this investigation, the maximum viscous correction is 2.5 per cent for a Reynolds number of 425.

The calibration curves for the recovery factor of a total-temperature probe are given, plus an analysis of suitable parameters with which to present this information. For the limited range of total-temperatures of 200°F to 260°F, and a nominal Mach number of 5.6, single calibration curves are shown using either the free-stream Reynolds number, or the Nusselt number of the flow inside the probe (based on thermocouple wire diameter) as parameters.

TABLE OF CONTENTS

NOMENCLATURE

a	speed of sound, ft./sec.
A	area, sq. ft.
A^*	area of a sonic throat, sq. ft.
c_p	specific heat at constant pressure, Btu/(lb.)(deg.F)
d	probe outside diameter, inches
d_i	probe inside diameter, inches
h	heat transfer coefficient, Btu/(sq. ft.)(deg. F)(sec.)
h	characteristic outside dimension for flattened probes, inches
J	constant conversion factor = 778 ft. lb./Btu
k	thermal conductivity, Btu/(ft.)(deg. F)(sec.)
ℓ	mean molecular free path length, inches
M	Mach number, u/a, dimensionless
M_p	Mach number inside temperature probe = constant
Nu	Nusselt number, hd/k, dimensionless
Nu^*	defined by $Nu\ k_g / \sqrt{M_p}\ k_w$, dimensionless
p	pressure, lbs./sq. in.
Pr	Prandtl number, $\mu\ c_p/k$, dimensionless
Q	heat flux, Btu/sec.
r	temperature recovery factor, dimensionless
R	gas constant for air = 1715 sq. ft./(sec.^{2})(deg. F)
Re	Reynolds number, $\rho\ ud/\mu$, dimensionless
Re^*	Reynolds number evaluated at total temperature
T	absolute temperature, deg. R
u	local velocity, ft./sec.

$\bar{v}$ mean molecular velocity, ft./sec.

x variable length, ft.

γ ratio of specific heats, c_p/c_v, dimensionless

λ a length of thermocouple wire, inches

μ absolute viscosity, lb. sec./sq. ft

ρ mass density, lb. $sec.^2/ft.^4$

Subscripts

$( )_g$ refers to gas conditions

$( )_o$ stagnation or reservoir conditions

$( )_w$ pertaining to the thermocouple wire

Superscripts

$( )'$ conditions after normal shock, for an inviscid fluid

$( )''$ stagnation conditions as read by impact-pressure probe

I. INTRODUCTION

Performance investigations of long-range missiles and rockets inevitably lead to the conclusion that hypersonic Mach numbers are required for efficient operation. This conclusion quite naturally directs attention to the complex aerodynamic problems associated with hypersonic flight in the upper atmosphere. To obtain basic aerodynamic information on bodies moving in this new regime, where the molecular mean free path lengths are appreciable compared with the characteristic body dimension, the hypersonic wind tunnel is an important tool. For purposes of identification, Mach numbers of 5 and above are considered, in this report, as comprising the "hypersonic" velocity range.

The problems involved in the accurate determination of local fluid stream properties, such as Mach number and Reynolds number, are much more difficult in a hypersonic wind tunnel than in supersonic or subsonic facilities of higher density. This difficulty stems primarily from the larger viscous effect encountered in the hypersonic wind tunnel. It is the purpose of this experimental investigation to calibrate and interpret impact-pressure and total-temperature measurements in a hypersonic air stream.

Impact-pressure interpretation in supersonic and subsonic flows of low density has been the subject of several theoretical and experimental investigations (Refs. 1 to 8). It seems desirable to determine to what extent the basic results of these previous investigations are applicable at higher Mach numbers.

When considering supersonic continuum flow of a compressible,

non-viscous fluid, the familiar Rayleigh formula (Cf. Ref. 9) is conventionally used to relate the observed impact pressure to the free stream static pressure and Mach number. However, as viscous forces become appreciable compared with inertia forces, the Rayleigh formula becomes increasingly inaccurate. Theoretical viscous corrections have been applied to the Rayleigh equation in Refs. 4 and 5 for selected impact-probe geometries.

The general field of rarefied gas dynamics, in which the analyses of continuum flow are no longer valid, is discussed by Tsien in Ref. 10. It is indicated in this reference that the ratio of the mean molecular free path length to a characteristic dimension of a body immersed in a fluid stream is a significant parameter for estimating the magnitude of the low-density effect. It is further established that this ratio, ℓ/d, is proportional to the Mach number divided by the Reynolds number. However, the magnitude of the ratio ℓ/d for which the methods of continuum flow mechanics are inadequate is not well defined. From experimental data obtained by Kane and Maslach (Ref. 2), it appears that conventional gas dynamics theory requires corrections for values of ℓ/d greater than about 0.015.

When the molecular mean free path becomes large with respect to the body dimensions, a free molecular flow exists. This regime of fluid mechanics is characterized by Tsien as having values of ℓ/d which are greater than 10 (Ref. 10). In this case, the molecules in the free stream can hit the body surface at full speed and be re-emitted without direct interference from other molecules. In fact, collisions of a molecule with the body are more frequent than collisions with

other molecules. Shock waves are no longer recognizable as such in a free molecular flow, and the kinetic theory of gases must be used to predict impact pressures.

Experimental investigations of impact pressure have been made in the Mach number range of 1.7 to 4.0, apparently in the transition region between continuum and free molecular flow, but near the estimated continuum limit (Refs. 1 and 2). Results of these investigations indicate that at very low Reynolds numbers the measured impact pressures are higher than those which would be computed from the Rayleigh formula. In addition, Ref. 1 indicates a region at slightly higher Reynolds numbers where the measured impact pressure is less than that predicted by the Rayleigh equation.

The impact-pressure phase of the present investigation involves experiments designed to determine the behavior of impact-pressure measurements at higher Mach numbers for two different impact-probe geometries. Practical considerations limited this investigation to a nominal Mach number of 5.6 and to a minimum Reynolds number of 425, based on impact-probe outside diameter and free stream conditions.

The design and calibration of total-temperature probes for use in hypersonic air streams have been considered in Ref. 11. Similar investigations of total-temperature probes have been conducted for subsonic and supersonic velocities (Cf. Refs. 12 and 13).

The design of a total-temperature probe involves a considerable amount of theoretical study and experimental investigation. The proper selection of materials and dimensions for the construction of a total-temperature probe is largely a qualitative process. Rather extensive

design and calibration studies of total-temperature probes at hypersonic velocities have been conducted by E. Winkler of the Naval Ordnance Laboratory.

The optimum calibration curve for displaying total-temperature data is one which would be valid for all flow conditions. It is not obvious, however, what fluid flow parameter will yield such an optimum calibration curve. The conventional parameters, Mach number and Reynolds number, have been used with reasonable success at subsonic and supersonic velocities, but in the hypersonic range use of one of these parameters as the variable will, as a general rule, yield families of calibration curves for constant values of the other parameter.

A parameter involving the Nusselt number of the flow inside the probe (based on thermocouple wire diameter) and the ratio of gas thermal conductivity to mean thermal conductivity of the thermocouple wires has been considered in Ref. 11. The temperature recovery factor for a given probe was plotted versus this parameter, and a single calibration curve was obtained which was valid for a considerable range of Mach numbers, Reynolds numbers, and stagnation temperatures. In justification of this parameter, an elementary heat balance analysis for a bare thermocouple wire was conducted during the present investigation and is included as Appendix A.

The scope of the temperature phase of this investigation did not include the design of a new total-temperature probe. Instead, it was determined to construct a temperature probe based on successful exisitng designs and then to calibrate this probe at a nominal Mach number of 5.6, over a range of free stream Reynolds numbers. Two total-temperature

probes based on designs suggested in Ref. 11 were constructed and compared, and the one yielding the highest recovery factor was calibrated for use in further investigations.

The experimental results presented in this paper were obtained in the GALCIT Hypersonic Wind Tunnel, Leg No. 1, in cooperation with LT N. R. Quiel, U. S. Navy, under the supervision of Dr. H. T. Nagamatsu.

II. EQUIPMENT AND PROCEDURE

A. Wind Tunnel Description

The GALCIT 5 x 5 inch Hypersonic Wind Tunnel (Leg No. 1) was used for these tests. It is of the continuously-operating, closed-return type and is operated by a compressor plant consisting of sixteen compressors driven by seven electric motors. The thirteen compressors in the first five compression stages are Fuller rotary compressors, while the final two stages consist of three reciprocating compressors. A system of valves and interconnecting piping permits the selection of a wide variety of plant compression ratios and mass flows. These valves, as well as the compressors, are operated remotely from a master control panel (Cf. Fig. 1). A schematic diagram of the wind tunnel installation is shown in Fig. 2.

The Leg No. 1 test section with fixed nozzle blocks designed for a nominal Mach number of 6 was used for these tests. The nozzle blocks were designed by the Foelsch analytical method with correction applied for the estimated boundary layer growth. Static orifices were provided at one-inch intervals in both nozzle blocks to permit a check to be made with the original nozzle calibration.

The Leg No. 1 air heating system employs superheated steam in a multiple pass heat exchanger and is capable of producing a maximum stagnation temperature of about 300°F at a reservoir pressure of 94 psia, and 230°F at atmospheric reservoir pressure.

The water content in the air was kept well below 100 parts per million (by weight) by passing it through a tank containing approxi-

mately 2000 pounds of silica gel. Oil was removed by Cyclone separators after each compression stage and, in addition, by finely-divided activated carbon canisters, porous carbon filter blocks, and a Mine Safety Appliances "Ultra-Aire Space Filter".

B. Model Description

1. Impact-Pressure Probe Rake

Six stainless steel probes, of varying diameter, were mounted on a 2 inch x 2½ inch stainless steel, wedge-shaped rake as shown in Fig. 3. The lead-in tubes, also of stainless steel, were completely enclosed within the wedge and its 5/16 inch diameter support rod. With the use of the externally-operated model control system in the tunnel test section, the rake could be moved vertically so as to bring each probe into the tunnel center line.

Two probe-end geometries were used. The Type I probes were sharp-lipped and circular-ended with outside diameters varying from 0.016 inch to 0.25 inch. The Type II probes were made by flattening the ends of round tubes so that the ratio of outside height to outside width was one-third. Sizes of probe-end outside heights ranged from 0.014 inch to 0.109 inch. Figure 4 shows a schematic sketch of these two probe geometries.

2. Stagnation-Temperature Probes

Two stagnation-temperature probes were constructed, both essentially similar to the design given in Ref. 11 but differing from each other in outside diameter of the probe entrance and thermocouple wire

diameter. Both probes consisted of a single platinum-coated quartz shield cemented to a stainless steel holder with a high-temperature ceramic cement. To replace continuously the air inside the probe, a single vent hole was provided in the shield aft of the thermocouple so that the vent-area to entrance-area ratio was approximately 1:5. Experimental data in Ref. 11 indicates that this area ratio is an optimum value. Iron-constantan thermocouples were cemented into a quartz support, which in turn was sealed into the stainless steel holder.

Probe A had an entrance outside diameter of 0.10 inch, and B. and S. gage 30 (.01 inch diameter) thermocouple wire was used, while the outside diameter of the entrance of Probe B was .063 inch, and 0.012 inch diameter thermocouple wire was used. Fig. 5 gives a schematic sketch of these probes, and Fig. 6 shows the probe support on which the probes were mounted for placement in the tunnel. It should be noted that this latter probe support also included an impact-pressure probe and a static-pressure probe, in addition to the temperature probe, so that flow conditions in the tunnel test section could be measured readily. Each probe could be positioned in turn on the tunnel center line by means of the model support control.

3. Static-Pressure Probe

The static-pressure probe was constructed of 0.083 inch outside diameter stainless steel tubing with a solid 10 degree conical nose. Three static orifices spaced uniformly around the tube circumference were located 30 diameters downstream from the nose.

C. Instrumentation

1. Pressure Measurements

The reservoir pressure was measured with a Tate-Emery nitrogen-balanced gage and controlled within ± 0.04 psi by a Minneapolis-Honeywell-Brown circular chart controller. All static and impact pressures were measured on a silicone fluid, vacuum-referenced manometer (Fig. 1). With the latter, pressures could be easily read to the closest 0.1 cm and estimated to 0.01 cm of silicone. This estimate is approximately equivalent to 0.07 microns of mercury.

2. Temperature Measurements

The tunnel stagnation temperature was measured by an iron-constantan, shielded thermocouple located one inch upstream from the nozzle throat and was recorded and controlled by a Minneapolis-Honeywell-Brown circular chart controller to within $\pm 2^{\circ}F$. The thermocouples in the stagnation-temperature test probes were differentially connected with the reservoir thermocouple to a Leeds and Northrup slide-wire potentiometer, as shown schematically in Fig. 7.

D. Test Procedure

1. Impact-Pressure Runs

Prior to the installation of the probe rake in the test section, an axial static pressure survey was conducted on the tunnel center line to locate a region of uniform pressure. A point 19.7 inches aft of the throat was selected, and the impact-pressure probe ends were aligned

accordingly. In addition, a vertical total-head survey was made at this position with results as shown in Fig. 8.

After the probe rake was installed and connected to the manometer, each complete system was carefully leak-checked. With the tunnel operating at a specified reservoir condition, each of the six different-sized probes on the rake was in turn placed at the test section center line, and its pressure measured on the silicone manometer. This positioning was accomplished with the vertical-actuating model control system, which was externally operated. In addition to counter readings on the vertical supports, it was found desirable to use the schlieren system and a fixed grid network placed on the glass port to check the center line positioning. The cycle was repeated until a determination of the reproducibility of results was completed.

Since it was desired to obtain the lowest possible Reynolds number (and consequently, the lowest air density) in the test section, the stagnation conditions of minimum possible stagnation pressure (p_o) with the corresponding maximum total temperature (T_o) were selected for one run. In addition, several runs at slightly lower T_o's and higher p_o's were made.

The actual reservoir temperature and pressure combinations used were as follows:

p_o(psia)	T_o(°F)	Remarks
14.7	230	one-phase flow
14.7	221	one-phase flow
14.7	210	one-phase flow
30.7	242	one-phase flow

A schlieren picture was taken of the flow around the probe rake to determine if any shock wave interference existed from one probe to another. Referring to Fig. 9, it is seen that the strongest shock wave, created by the largest probe, does not intersect the adjacent probe until it is many diameters downstream.

2. Total-Temperature Runs

The total-temperature probe was mounted in the tunnel on a support which also included a total-pressure probe and a static-pressure probe as shown in Fig. 6. The latter two probes were connected to the manometer system and then carefully leak-tested. The leads from the test thermocouple were differentially connected with the reservoir thermocouple to the potentiometer. Thus, the e.m.f. read on the potentiometer was proportional to the temperature difference between T_o and the temperature sensed by the test probe, T_o'.

For each calibration run, the reservoir temperature was held fixed and the reservoir pressure varied throughout its possible range. At each flow setting the total pressure, static pressure, and e.m.f. were recorded.

III. REDUCTION AND ANALYSIS OF DATA

A. Impact-Pressure Correction Technique

In order to determine a viscous correction, it is first necessary to find the value which the impact pressure would have if the flow were essentially inviscid. This value could be determined if an impact probe were used which was sufficiently large that the viscous effects were no longer detectable. However, it was not known intuitively whether the Reynolds number of the largest probe on the probe rake tested was large enough to be free of viscous effects. Consequently, some additional analysis was necessary.

A method of attack which proved quite satisfactory in Ref. 1 was employed. This technique consisted of plotting the measured impact pressures against the inverse of impact-probe diameters for the six different-sized probes tested and extrapolating a curve through the resulting points to $1/d = 0$. The value of the pressure intercept at this point was considered to be that corresponding to the impact pressure in an inviscid fluid.

This process of letting $1/d$ approach zero was considered equivalent to letting the Reynolds number approach infinity, all other factors in Re having been held constant. Typical plots of data involving this process are shown in Fig. 10.

B. Determination of Flow Parameters

1. Mach Number

With the measured impact pressure, corrected for viscous effects as explained previously, plus the measured static pressure, the free

stream Mach number was calculated using Rayleigh's well-known supersonic pitot tube equation. In the instance where the static pressure was measured during a run subsequent to a series of impact-pressure runs, the reproducibility of flow conditions was checked by means of a reference impact-pressure probe.

The subsonic Mach number of the flow within the total-temperature probes was calculated simply from the area ratio of the shield inside diameter to the vent. Since the pressure ratio at the vent, p/p_o', is well below the critical value, a sonic throat exists in the vent passage. Thus, for a given probe geometry, the Mach number of the flow within the probe is essentially independent of free stream flow conditions.

2. Reynolds Number

The Reynolds number per inch based on undisturbed free stream conditions was calculated for each flow setting. The corresponding Reynolds number for each impact probe based on the outside diameter was then determined. The measured free stream pressure, the stagnation temperature, and the corresponding value of the Mach number were used to compute the Reynolds number.

By definition we can write

$$Re = \frac{\rho u d}{\mu} = \frac{\rho M a d}{\mu} \tag{1}$$

The assumption of the perfect gas law gives $\rho = p/RT$, and the sonic velocity, a, is given by $a = \sqrt{\gamma RT}$. Substituting for ρ and a in Eq. (1) we obtain

$$Re = \frac{M \sqrt{\gamma RT}\, pd}{\mu RT} \tag{2}$$

which reduces to

$$Re = 0.343 \frac{p M d}{\mu \sqrt{T}} \tag{3}$$

for $\gamma = 1.4$ and $R = 1715$ ft./sec.^{2} $^\circ$R. The units of p, d, u, and T are given in the list of symbols.

By assuming adiabatic flow the free stream temperature, T, was then obtained from the equation

$$T = \frac{T_o}{1 + \frac{\gamma - 1}{2} M^2} \tag{4}$$

A plot of this equation given in Ref. 14 was used.

The corresponding value for the viscosity of air was obtained from a plot of the Keyes' equation for viscosity. Ref. 15 indicates that for air at very low temperatures Keyes' equation is more appropriate than the familiar Southerland's equation for viscosity. For air, Keyes' equation becomes

$$\mu \text{ (slugs/ft. sec.)} = 2.316 \times 10^{-10} \frac{\sqrt{T}}{1 + \frac{219.8}{T} 10^{-9/T}} \tag{5}$$

At higher temperatures (above 500°R) the viscosity for air was obtained from curves based on Southerland's equation given in Ref. 16.

Thus, all the properties used to characterize the air stream have been those of the undisturbed free stream. It was also desired to obtain a set of reference properties based on conditions behind a normal shock wave. The change in properties of a free stream passing through a normal shock wave was calculated by the use of curves of normal shock wave functions given in Ref. 14.

3. Knudsen Number

The mean molecular free path lengths for the undisturbed free stream and for flow conditions after a normal shock wave were calculated. For each probe the corresponding Knudsen numbers were determined. From Kinetic theory, Chapman gives (Ref. 17)

$$\mu = 0.499 \rho \bar{v} \ell \tag{6}$$

where $\bar{v}$ is the mean molecular speed and ℓ is the mean molecular free path length. Results from kinetic theory also connect $\bar{v}$ with the velocity of sound, a, by

$$\bar{v} = \sqrt{\frac{8}{\pi \gamma}}\ a \tag{7}$$

where γ is the ratio of specific heats. Combining Eqs. (6) and (7) yields

$$\ell = \frac{0.499\ \mu}{\rho a}\ \sqrt{\frac{\pi \gamma}{8}} \tag{8}$$

Noting that $\mu/\rho a = Md/Re$ and using $\gamma = 1.4$ for air, Eq. (8) becomes

$$\ell = 1.49\ (M/Re)\ d \tag{9}$$

The Knudsen number is now expressed as a function of Reynolds number and Mach number:

$$\ell/d = 1.49\ (M/Re) \tag{10}$$

4. Nusselt Number

The Nusselt number considered here involves the rate of heat transfer between the air flow and the thermocouple wire. It is defined in general by

$$Nu = \frac{h\, d_w}{k_g} \tag{11}$$

where h = heat transfer coefficient

k_g = gas thermal conductivity

d_w = thermocouple wire diameter

Moreover, for flow in which heat transfer is taking place we may write

$$Nu = f_1(M, Re, Pr) \tag{12}$$

where Pr is the Prandtl number for air and may be considered as remaining constant. Now, if we determine the Reynolds number, Re^*, based on an evaluation of gas density and viscosity at total temperature rather than at static temperature, then

$$Re^* = g(Re, M) \tag{13}$$

and so

$$Nu = f_2(Re^*) \tag{14}$$

In Ref. 18, a semi-empirical equation has been determined for this relation, namely,

$$Nu = 0.431 \sqrt{Re^*} \tag{15}$$

With this equation the Nusselt number of the flow inside the total-

temperature probe (based on thermocouple wire diameter) is easily calculated from measured quantities as follows:

$$Re^* = \frac{\rho_o V_p d_w}{\mu_o} = \frac{0.343\, p_o' M_p d_w \sqrt{T}}{T_o \mu_o}$$

$$Re^* = \frac{0.343\, p_o' M_p d_w}{\sqrt{T_o}\, \mu_o (1 + 0.2 M_p^2)^{\frac{1}{2}}} \tag{16}$$

where

p_o' = impact pressure in lbs./in.^{2}

μ_o = $f(T_o)$ = gas viscosity in lbs./ft.^{2}-sec.

d_w = thermocouple wire diameter in inches

M_p = Mach number inside probe

For the given probe geometries considered, there exists the problem of determining the proper area ratio to use in calculating M_p. However, considering the entrance area, where M_p is even greater than it is at the thermocouple wire, we find

$$A/A^* = 5 \quad , \quad M_p = 0.117$$

Thus, the variation of the denominator of Eq. (16) with M_p is negligible, and we can write

$$\frac{Re^*}{M_p} = \frac{0.343\, d_w p_o'}{\sqrt{T_o}\, \mu_o} \tag{17}$$

where the indefiniteness of calculating the constant M_p is eliminated by including it with the parameter Re^*.

From experimental results in Ref. 11 and an analysis of heat transfer balance in the thermocouple wire contained in Appendix A, it appears that the parameter $Nu\ k_g/k_w$ is significant for the investigation of the temperature recovery factor. Accordingly, a parameter Nu^* is defined

$$Nu^* = \frac{Nu\ k_g}{\sqrt{M_p}\ k_w} \tag{18}$$

Using Eqs. (15) and (17), this may be written

$$Nu^* = \frac{0.252\ d_w^{\frac{1}{2}}\ p_o'^{\frac{1}{2}}\ k_g}{T_o^{\frac{1}{4}}\ \mu_o^{\frac{1}{2}}\ k_w} \tag{19}$$

For the thermocouple, k_w is a constant and may be considered as the mean of the two values for iron and constantan. However, k_g varies with the changing conditions of the gas. In Ref. 18, a suggested formula for calculating k_g is

$$k_g = 3.03 \times 10^{-8}\ T^{0.78} \tag{20}$$

Thus, for a given probe geometry, Nu^* is dependent only on the local reservoir conditions; and for any given run at a constant T_o, Nu^* is a function only of impact pressure, p_o'.

C. Temperature Recovery Factor Determination

In order to calibrate a total-temperature probe for future application, some measure of its ability to convert all of the kinetic energy of an air stream into heat energy must be obtained. For this

purpose a temperature "recovery factor" is commonly defined as

$$r = \frac{T_o' - T}{T_o - T} \tag{21}$$

where T_o' is the temperature sensed by the probe.

Since it was desired to measure as accurately as possible the small difference between T_o and T_o', the probe thermocouple was differentially connected with the reservoir thermocouple, as shown in Fig. 7. In this manner, the e.m.f. read on the potentiometer was proportional to the difference, $T_o - T_o'$. Using the thermocouple temperature-millivolt equivalent, the temperature difference was converted to degrees Fahrenheit.

With the recording of reservoir temperature, T_o, and subsequent calculation of the stream temperature, T, using the adiabatic energy equation, all information for determining recovery factor was available.

IV. EXPERIMENTAL RESULTS AND DISCUSSION

A. Impact-Pressure Measurements

1. General Results

Two types of probes, as shown in Fig. 4, were tested at a nominal Mach number of 5.6. The complete range of free stream conditions used are summarized as follows:

$$M = 5.3 \text{ to } 5.6$$

$$Re = 425 \text{ to } 8000$$

$$\ell/d = 0.001 \text{ to } 0.018$$

where the Reynolds numbers are based on the outside diameter of the probes.

The primary results of impact-pressure measurements for Type I probes are presented in Figs. 11 to 14, while similar presentations for Type II probes are contained in Figs. 15 and 16. There are two curves for each probe, based on two different free stream parameters, each showing the ratio of measured impact pressures to the ideal non-viscous impact pressure. In addition, two curves are presented for Type I probes based on flow conditions behind a normal shock. These results show that the Rayleigh supersonic pitot tube equation requires correction for viscous effects when the Reynolds number of the undisturbed free stream becomes less than about 6000. It should be noted, however, that these specific corrections apply to particular type probes and a restricted Mach number range.

The maximum deviation of the measured impact pressure from the

ideal impact pressure was 2.5 per cent. This maximum deviation was obtained at the lowest Reynolds number attainable with the experimental equipment used, and it appears from the shape of the curves in question that this deviation would become larger with decreasing Reynolds number. All of the deviations of the measured impact pressures from the ideal, non-viscous, impact pressure were negative (i.e., $p_o''/p_o' < 1$).

2. Choice of Parameters Used to Present the Data

The variations of the measured impact pressure from that predicted by the Rayleigh equation are apparently due to viscous forces. Consequently, it would seem that an appropriate parameter for presenting the impact pressure ratios would be Reynolds number, based on either flow conditions ahead of or behind a normal shock. If the Reynolds number based on the undisturbed flow is chosen as the parameter, it would be expected that the curves of impact-pressure ratio versus Reynolds number would not be independent of Mach number.

Another parameter which is a significant measure of the effects of viscous forces associated with low densities is the Knudsen number, or $\ell/d \sim M/Re$. It is not known, however, to what extent this parameter would yield a pressure deviation curve that is independent of Mach number. Unfortunately, practical considerations circumvented the original intention to include a considerably higher Mach number range in this investigation.

Presentations of the data versus parameters, based on stream conditions behind a normal shock, are included to permit comparison with results for impact-pressure corrections in subsonic flows.

3. Comparison with Previous Experimental Investigations and Theory

The present investigation was conducted at a considerably higher Mach number than any known previous work. Hence, it is only possible to compare the results qualitatively. Perhaps the most significant difference in results obtained in this investigation as compared with previous investigations at lower Mach numbers is the detection of viscous effects at much higher Reynolds numbers. For instance, the results of Ref. 1 for a nominal Mach number of 2.5 do not indicate viscous effects in the impact pressure until the Reynolds number has decreased to about 200, while the present results at a nominal Mach number of 5.6 show viscous effects at Reynolds numbers as high as 6000.

For a probe similar to Type I, the results of Ref. 1 show a negative pressure variation (that is, with the measured impact pressures less than the ideal value) in the Reynolds number range from 30 to 200 and a positive pressure variation at Reynolds numbers below 30. The results of the present investigation are qualitatively in agreement with those in Ref. 1, since it is entirely possible that the curves in Figs. 11 and 15, for example, would swing up to positive values of p_o''/p_o' if data at lower Reynolds numbers were available at this Mach number.

Ref. 2 presents some impact pressure data versus the parameter M/Re for a source-shaped probe, which is found in Ref. 1 to have considerably different viscous characteristics than those of Type I in this report. Moreover, no results with the parameter M/Re are given in Ref. 1. Consequently, it is difficult to reach any definite conclusions regarding the suitability of the parameter $\ell/d \sim M/Re$. However, a few conversions of data from Ref. 1 at a nominal Mach number of 2.5 indicate very little to substantiate a favorable comparison.

A theoretical development which predicts a viscous correction for impact pressure in a supersonic, continuum, viscous flow is contained in Ref. 5. The analysis assumes a stagnation line flow through a normal shock wave and includes the viscous effects in the subsonic flow field by means of a boundary layer theory. The theory developed predicts that the pressures sensed by an impact probe in a viscous fluid will always be larger than the pressure so obtained in a non-viscous fluid.

This theory is at variance with the experimental results recorded in the present investigation but is in agreement with previous investigations at lower Mach numbers, at particular ranges of Reynolds numbers, and with certain other probe geometries. It appears, therefore, that the theory is only valid for certain probe geometries, over particular Mach number and Reynolds number ranges.

Another theoretical analysis, contained in Ref. 8, is based on entropy rise and the related energy dissipation behind a detached normal shock wave. This development predicts that measured impact pressures in a viscous, supersonic flow are less than the ideal non-viscous impact pressure. For the range of Mach numbers and Reynolds numbers of the present experimental investigation, it appears that this theoretical analysis more closely describes the physical phenomenon.

B. Total-Temperature Probe Calibration

1. Initial Calibrations for Comparison of Probes A and B

The initial calibrations were conducted at a constant total temperature of 225°F. The choice of this temperature was based on two considerations: it was sufficiently high to avoid condensation of

constituents of the air in the wind tunnel test section, and it could be maintained over the entire operational range of reservoir pressures. Over the range of test conditions, the Mach number tended to decrease slightly with decreasing reservoir pressure and increasing reservoir temperature. This Mach number variation was due to unavoidable variation of boundary layer thickness in the nozzle. Test conditions for these initial calibrations are summarized as follows:

p_o(psia)	=	14.7	to	94.7
Re/inch	=	30,800	to	213,000
M	=	5.5	to	5.8

Primary results of these calibrations are presented in Fig. 17. The variation of temperature recovery factor with Reynolds number is plotted for the two probes. The Reynolds numbers refer to free stream conditions and are based on the outside diameter of the entrance to the probe. Adiabatic flow from the temperature probe located just ahead of the nozzle throat to the total temperature probe in the test section was assumed.

The over-all shape of the two calibration curves is similar. However, the recovery factor for Probe B is considerably lower than that for Probe A. This difference can be partially attributed to the smaller entrance diameter of Probe B. Evidently, the smaller diameter shield allows more conduction and radiation losses from the stagnation streamline than does the larger shield. In addition, the shield on Probe B is somewhat longer than that on Probe A. The increased shield length is also conducive to more heat loss. The length over diameter ratios of the

thermocouple wires for the two probes are essentially the same. Hence, it would be expected that the conduction loss through the thermocouple wires would be approximately the same for the two probes.

In view of the relatively poor performance of Probe B, no additional calibrations were made of this temperature probe at other reservoir temperatures; instead, only probe A was used for more extensive calibration analysis.

2. Extended Calibration of Probe A

In addition to the initial run at a constant reservoir temperature of 225°F, Probe A was also calibrated at total temperatures of 200°F and 260°F, over the complete operating range of reservoir pressures. Thus, three sets of data were recorded for essentially the same range of Reynolds numbers and Mach number, which were as follows:

$$\text{Re/inch} = 30{,}800 \text{ to } 213{,}000$$
$$M = 5.5 \text{ to } 5.8$$

The results of the calibration of Probe A are contained in Figs. 18, 19, and 20. Temperature recovery factor is plotted versus the three different parameters, Re, Nu, and Nu^*, in an attempt to investigate the effect of total-temperature variation at constant Mach number. However, for the limited total-temperature range available, any effect on the Re and Nu curves due to change in total temperature is not distinguishable within the normal scatter of experimental data as seen in Figs. 18 and 19. This is somewhat at variance with data presented in Ref. 11, where it was found that for Reynolds numbers below 20,000 the calibration curves for different total temperatures began to diverge quite appre-

ciably and continued to diverge with decreasing Reynolds number. Some of this discrepancy may be accounted for by the fact that in Ref. 11 the total temperature changes were greater and, therefore, the divergences more readily detected.

3. Suitability of Parameters for Presenting Temperature Recovery Factor Calibrations

The ideal parameter to use in plotting a calibration curve is one that would yield a single curve valid over a considerable range of flow conditions. Results of this investigation indicate that for a constant Mach number, either the free stream Reynolds number or the Nusselt number based on flow conditions inside the probe and on thermocouple wire diameter produces a single curve. It is difficult, however to justify theoretically the significance of these parameters in this respect and they could not be expected to retain this property for variable Mach numbers.

From a consideration of a simplified theory of heat transfer and the assumption that heat losses other than conduction through the thermocouple wires are negligible, it would appear that the recovery factor, when plotted versus Nu^* (defined by Eq. 18), should be invariant with total temperature and free stream Mach number. The theoretical analysis in Appendix A indicates the significance of the parameter $Nu\ k_g/k_w$, which is proportional to Nu^*, this factor of proportionality being constant for a given probe geometry.

Referring to Fig. 20, it is seen that the use of this parameter, Nu^*, does not yield a single calibration curve as effectively as does

that of the other two parameters considered. It thus appears that the assumptions made in Appendix A are perhaps over-simplified and do not provide an adequate analysis for the temperature probe used in this investigation. It is believed, however, that for variable free stream Mach numbers, this parameter would prove superior. In Ref. 11, a single calibration curve was actually obtained for a variety of different total temperatures, Reynolds numbers, and Mach numbers, using the parameter Nu k_g/k_w, which is, as mentioned previously, proportional to what is defined here as Nu^*.

It should be noted that the Nusselt number of the flow within a given probe geometry is particularly convenient to use. The only data needed are the total temperature and the impact pressure.

V. CONCLUSIONS AND RECOMMENDATIONS

The results of the impact-pressure phase of this investigation provided the following evidence as to the interpretation of measured impact pressures at a nominal Mach number of 5.6:

(1) Viscous effects on impact-pressure measurements are encountered at Reynolds numbers as high as 6000. These effects are such as to cause the measured impact pressure to read lower than predicted by the Rayleigh formula.

(2) Within the range of this investigation, these viscous effects increase with decreasing Reynolds number, and at a Reynolds number of 425 the measured impact pressure is approximately 2.5 per cent lower than that predicted by the Rayleigh formula.

(3) A comparison with previous investigations at lower Mach numbers indicates that these viscous effects have a definite dependence on Mach number as well as Reynolds number.

(4) The flattened-end type of probe is more sensitive to the effects of viscosity than is the sharp-lipped circular type.

The results of the total-temperature phase of this investigation for a nominal Mach number of 5.6 and a reservoir temperature range of 200°F to 260°F are as follows:

(1) A comparison of two total-temperature probes indicates that the thermocouple shield with the largest entrance diameter and the shortest distance from its entrance to the thermocouple has the best temperature recovery factor.

(2) For the range of reservoir temperatures investigated, a single calibration curve has been obtained using either the Reynolds

number of the free stream based on the probe entrance outside diameter or the Nusselt number of the flow inside the probe based on thermocouple wire diameter.

It appears highly desirable that this impact-pressure investigation should be extended to higher Mach numbers and lower Reynolds numbers, since both of these variations tend to increase the viscous effects. In addition, it seems desirable to extend the total-temperature investigation to higher Mach numbers, lower Reynolds numbers, and a wider range of reservoir temperatures.

REFERENCES

1. Sherman, F. S.: "New Experiments on Impact-Pressure Interpretation in Supersonic and Subsonic Rarefied Air Streams", NACA TN 2995, 1953.

2. Kane, E. D. and Maslach, G. J.: "Impact-Pressure Interpretation in a Rarefied Gas at Supersonic Speeds", NACA TN 2210, 1950.

3. Kane, E. D. and Schaaf, S. A.: "Viscous Effects on Impact Probes in a Subsonic Rarefied Gas Flow", Report No. HE-150-82, Univ. of California, March 9, 1951.

4. Chambre, P. L. and Smith, H. R.: "The Impact Tube in a Viscous Compressible Gas", Report No. HE-150-63, Univ. of California, August 29, 1948.

5. Chambre, P. L.: "The Theory of the Impact Tube in a Viscous Compressible Gas", Report No. HE-150-50, Univ. of California, November 1, 1948.

6. Chambre, P. L. and Schaaf, S. A.: "The Theory of the Impact Tube at Low Pressures", Jour. Aero. Sci., Vol. 15, No. 12, December 1948, pp. 735-737.

7. Murphy, S.: "Evidences of an Inherent Error in Measurement of Total-Head Pressure at Supersonic Speeds", Aero. Eng. Review, vol. 12, No. 11, November 1953, pp. 47-51.

8. Staros, B.: "Investigation of Effect of Energy Dissipation Behind a Detached Shock Wave on Total-Head Measurements", Ae.E. Thesis, California Institute of Technology, 1950.

9. Liepmann, H. W. and Puckett, A. E.: "Introduction to Aerodynamics of a Compressible Fluid", John Wiley and Sons, Inc., New York, 1947.

10. Tsien, H. S.: "Superaerodynamics, Mechanics of Rarefied Gases", Jour. Aero. Sci., Vol. 13, No. 12, December 1946, pp. 653-664.

11. Winkler, E. M.: "Design and Calibration of Stagnation Temperature Probes for Use at High Supersonic Speeds and Elevated Temperatures", Jour. of App. Physics, Vol. 25, No. 2, 231-232, February 1954.

12. Goldstein, D. L. and Scherrer, R.: "Design and Calibration of a Total-Temperature Probe for Use at Supersonic Speeds", NACA TN 1885, 1949.

13. Hottel, H. C. and Kalitinsky, A.: "Temperature Measurements in High-Velocity Air Streams", Jour. of App. Mech., March 1945, pp. A25-A32.

14. Hypersonic Wind Tunnel Staff: "Charts and Tables for Analysis of Hypersonic Flow", California Institute of Technology, Guggenheim Aeronautical Laboratory, Hypersonic Wind Tunnel Memorandum No. 4, May 1951.

15. Eimer, M.: "Direct Measurement of Laminar Skin Friction at Hypersonic Speeds", Ph.D. Thesis, California Institute of Technology, 1953.

16. Morey, F. C.: "NBS-NACA Tables of Thermal Properties of Gases", Table 2.39, December 1950.

17. Chapman, S.: "On the Law of Distribution of Molecular Velocities, and on the Theory of Viscosity and Thermal Conduction, in a Non-Uniform Simple Monatomic Gas", Phil. Trans. Roy. Soc., Vol. 216(A), pp. 279-348, 1915.

18. Scadron, M. D. and Warshawsky, I.: "Experimental Determination of Time Constants and Nusselt Numbers for Bare-Wire Thermocouples in High-Velocity Air Streams and Analytical Approximation of Conduction and Radiation Errors", NACA TN 2599, 1952.

APPENDIX A

TEMPERATURE ERROR AT A THERMOCOUPLE JUNCTION DUE TO CONDUCTION IN THE THERMOCOUPLE WIRES

If it were possible to bring a fluid stream to rest adiabatically at a thermocouple junction, the kinetic energy of the stream would be completely recovered, and the fluid temperature at the junction would be the total temperature, T_o. With an actual temperature probe, it is impossible to achieve absolute adiabatic deceleration of the flow to stagnation. As the temperature of a fluid element in the stagnation streamline increases above the static temperature of the free stream, there is a loss of heat from the sample due to conduction of heat through the gas in addition to radiation and convective heat transfer to the probe shield.

However, according to Ref. 18, the heat loss due to non-adiabatic flow along the stagnation streamline and the heat loss from the thermocouple junction by radiation are considered to be relatively small compared to the heat loss from the junction by conduction through the thermocouple wires. Consequently, for this analysis, only the heat loss due to conduction through the thermocouple wire is considered. To evaluate this effect it is assumed that there exists a uniform fluid temperature, T_o, along the bare thermocouple wire and that there is a negative temperature gradient from the thermocouple junction to the base of the wire. It is also assumed that the temperature of the wire is constant at any cross section.

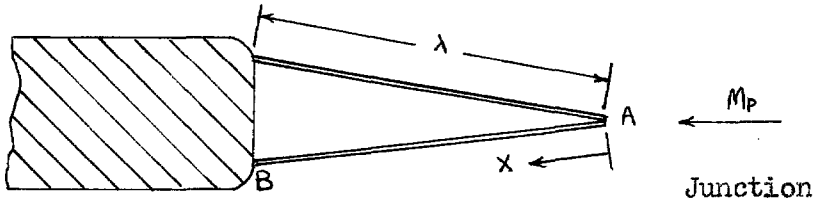

Referring to the above sketch, the temperature of the wire at A, T_A, must be greater than the temperature at B, T_B, in order for heat to flow from A to B. Also, $(dT/dx)_A = 0$ by symmetry, and the velocity inside the probe, u_p, is assumed small so that $(u_p^2)/(2g\ J\ C_p\ T_o) << 1$.

Considering an element of wire of length dx, the heat flux, Q, through the wire at a given cross section is

$$Q = \left(- \frac{d\ T_w}{dx} \right) k_w \frac{\pi d_w^2}{4} \qquad \text{(A-1)}$$

where k_w is the coefficient of thermal conductivity of the wire. Then at a point a distance, dx, from the given cross section the heat flux is given by

$$Q + dQ = - \left[\left(\frac{d\ T_w}{dx} \right) + \left(\frac{d^2\ T_w}{dx^2} \right) dx \right] k_w \frac{\pi d_w^2}{4} \qquad \text{(A-2)}$$

and the increment of heat flux in the element of wire of length dx is

$$dQ = - \frac{d^2 T_w}{dx^2} dx \; k_w \; \frac{\pi d_w^2}{4} \tag{A-3}$$

Now consider the heat flux from the fluid to the wire through the surface of the wire element. This may be written

$$dQ = (T_o - T_w) \; h \; \pi \; d_w \; dx \tag{A-4}$$

where T_o is the stagnation temperature of the fluid, $T_w(x)$ is the local temperature of the wire, and h is the convective heat transfer coefficient which includes the combined effect of conduction through the film and convection in the fluid. This coefficient is assumed to be constnat over the length of the wire.

Now, for equilibrium conditions to exist in the wire, the heat flux through the surface must equal the change of heat flux along the thermocouple wire. Thus, the resulting differential equation is

$$\frac{d^2 T_w}{dx^2} - \frac{4h}{k_w \, d_w} (T_w - T_o) = 0 \tag{A-5}$$

It is convenient now to introduce the Nusselt number, in the form

$$Nu = h \, d_w / k_g \tag{A-6}$$

where k_g is the coefficient of thermal conductivity of the fluid. Then, denoting the cross sectional area of the wire by A, Eq. (A-5) becomes

$$\frac{d^2 T_w}{dx^2} - Nu \; \frac{k_g}{k_w} \; \frac{1}{\pi A} \; (T_w - T_o) = 0 \tag{A-7}$$

The general solution of this differential equation is

$$T_w - T_o = c_1 e^{-\beta x} + c_2 e^{\beta x} \tag{A-8}$$

where

$$\beta^2 = Nu\,(k_g/k_w)(1/\pi A) \tag{A-9}$$

Now, if the boundary conditions are applied

$$c_1 = c_2 = \frac{T_B - T_o}{e^{-\beta\lambda} + e^{\beta\lambda}} \tag{A-10}$$

and

$$T_o - T_w = \frac{(T_o - T_B)\cosh \beta x}{\cosh \beta\lambda} \tag{A-11}$$

where λ is the length of wire between points A and B in the previous sketch. At the thermocouple junction, $x = 0$, $T_w = T_o'$, and Eq. (A-11) becomes

$$T_o - T_o' = \frac{T_o - T_B}{\cosh\ (\beta\lambda} \tag{A-12}$$

The energy equation for adiabatic, frictionless, steady flow of a perfect gas may be written

$$T_o - T = \frac{u^2}{2g\ J\ c_p} \tag{A-13}$$

and by the use of the definition of the temperature recovery factor, r, at the thermocouple junction, this equation becomes

$$T_o' - T = r\ \frac{u^2}{2g\ J\ c_p} \tag{A-14}$$

or

$$T_B - T = r_B \frac{u^2}{2g\ J\ c_p} \tag{A-15}$$

where r_B is the temperature recovery factor of the thermocouple base (Point B).

Combining Eqs. (A-12), (A-14), and (A-15) yields the following expression for recovery factor

$$r = 1 - \frac{(1 - r_B)}{\cosh \beta\lambda} \tag{A-16}$$

It is clear that for a given probe geometry, $r = r(r_B, \beta)$, where β is defined in Eq. (A-9). Thus, the significance of the parameter Nu (k_g/k_w) can be easily seen.

APPENDIX B

ACCURACY ANALYSIS OF EXPERIMENTAL DATA

The magnitude of the random errors encountered were estimated by considering the reproducibility of the observations, the sensitivity of the scale, and the associated reading error. For the experimentally measured quantities, these estimated errors are as follows:

Measurement	Estimated Maximum Error
Static pressure - p	± 0.2 mm. of silicone
Impact pressure - p_o''	± 0.5 mm. of silicone
Reservoir pressure - p_o	less than 0.5%
Reservoir temperature - T_o	$\pm 2^{\circ}F$
Thermocouple voltage	± 0.01 micro volt
Impact tube dimension d,h	$\pm .0005$ inch

The ideal impact pressure was obtained by an extrapolation procedure as explained in Section III. The estimated maximum probable error in the extrapolated value of impact pressure is ± 0.5 mm. of silicone. This estimated value was determined as a result of a graphical study of the extrapolation curves.

The accuracy of the computed values, based on both estimated errors in the individual measurements and the errors from the use of graphs, tables, etc., is as follows:

Quantity	Maximum Error
Ratio of impact pressures - P_o''/P_o'	± 0.12%
Mach Number - M	± 1%
Free Stream Temperature - T	± 2%
Reynolds Number - Re	± 5.5%
Temperature Recovery Factor - r	± .06%

LIST OF FIGURES

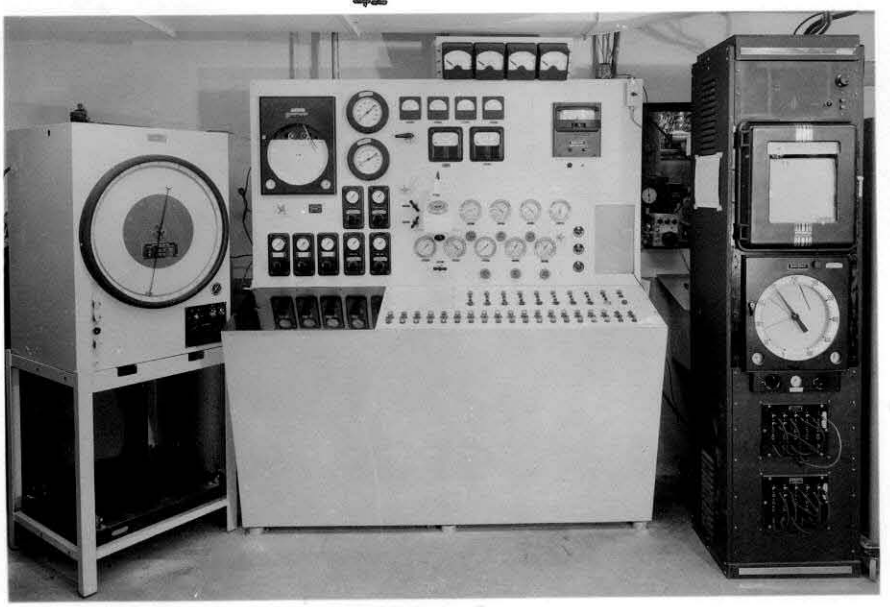

Compressor Plant Motor and Valve Controls
Reservoir Pressure and Temperature Regulators
Plant Pressure and Temperature Indicators

Fig. 1a

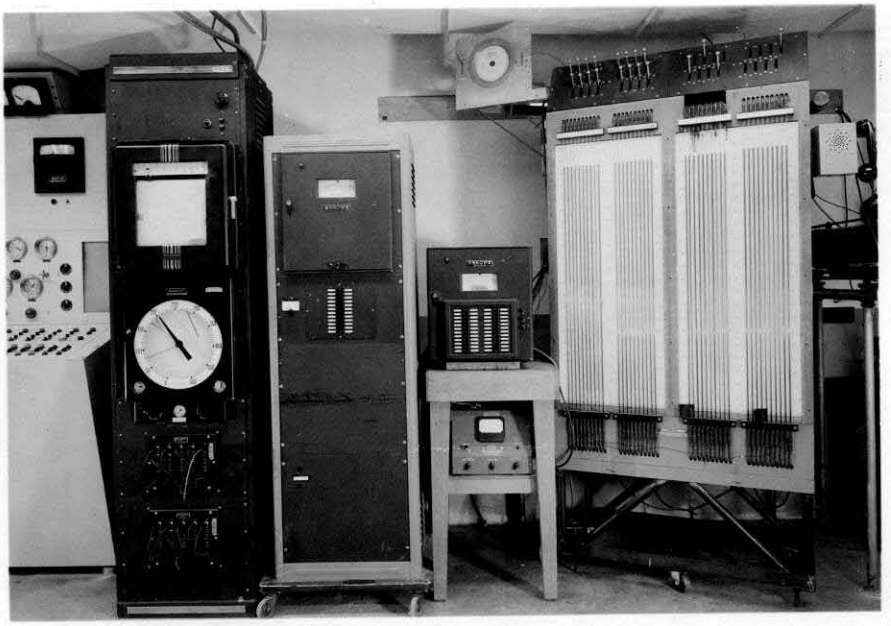

Test Section and Nozzle Block
Pressure and Temperature Instrumentation

Fig. 1b

GALCIT 5 x 5 IN. HYPERSONIC WIND TUNNEL
CONTROLS AND INSTRUMENTATION

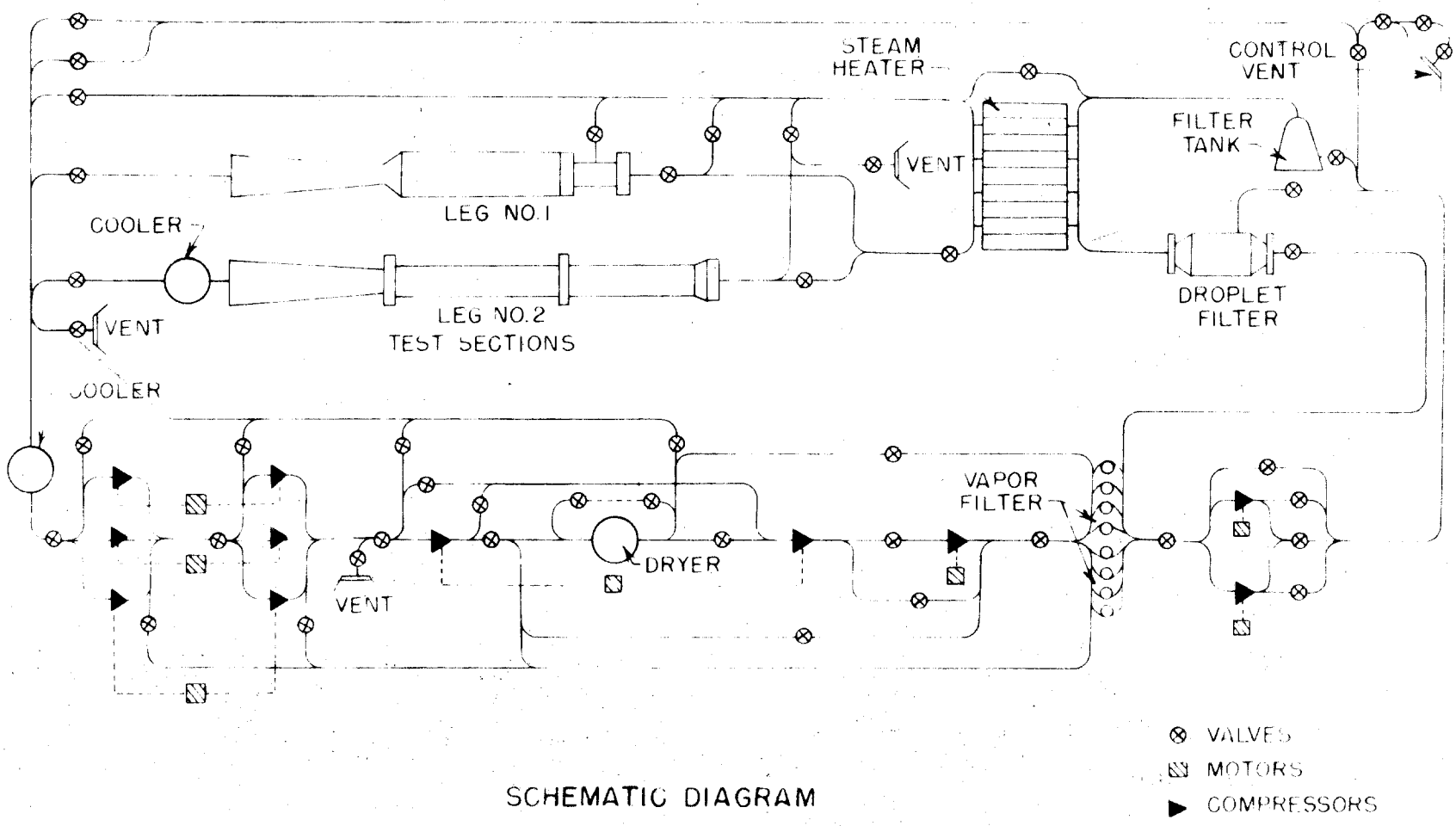

SCHEMATIC DIAGRAM

OF GALCIT 5x5in HYPERSONIC WIND TUNNEL INSTALLATION

FIG.2

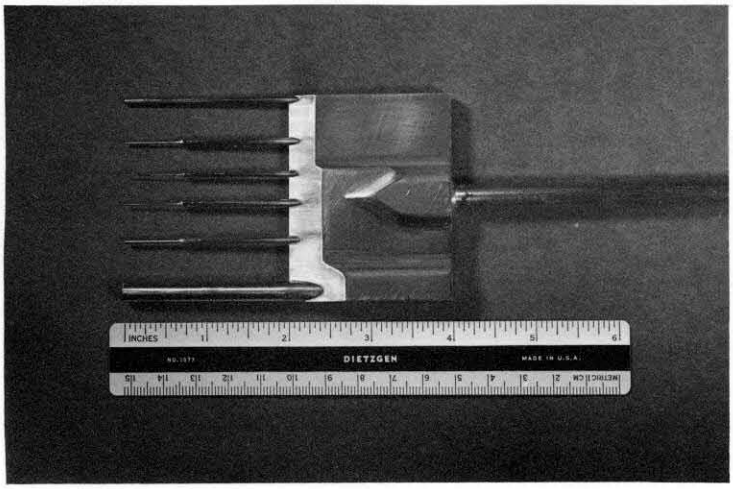

Type I Probes

Fig. 3a

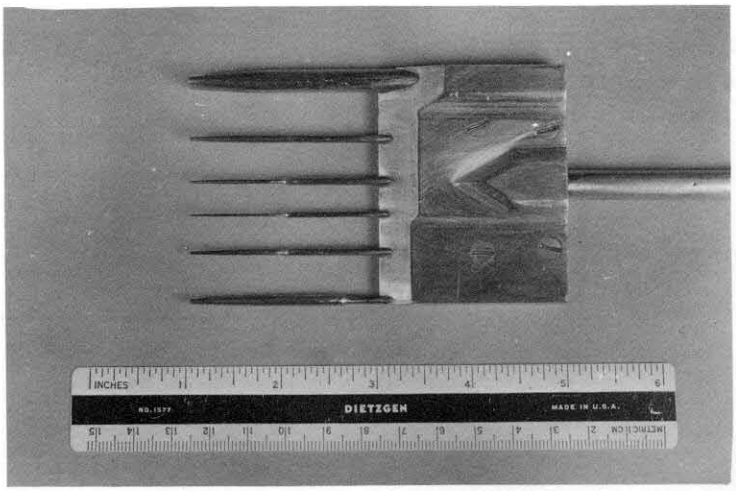

Type II Probes

Fig. 3b

IMPACT-PRESSURE PROBE RAKE

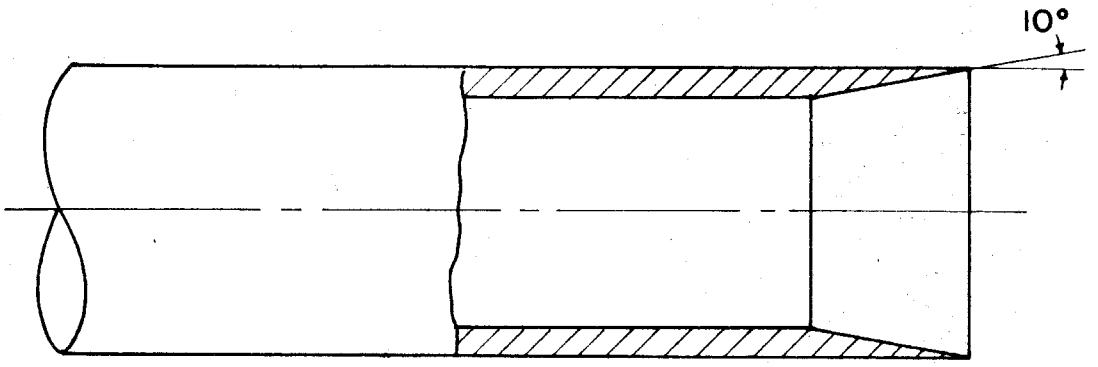

TYPE I - CIRCULAR-END TUBE

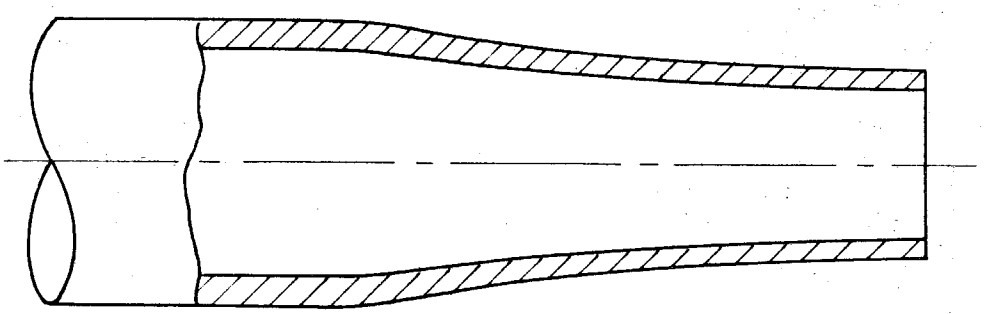

TYPE II - FLATTENED-END TUBE

SKETCH OF IMPACT-PRESSURE PROBE GEOMETRY

FIG. 4

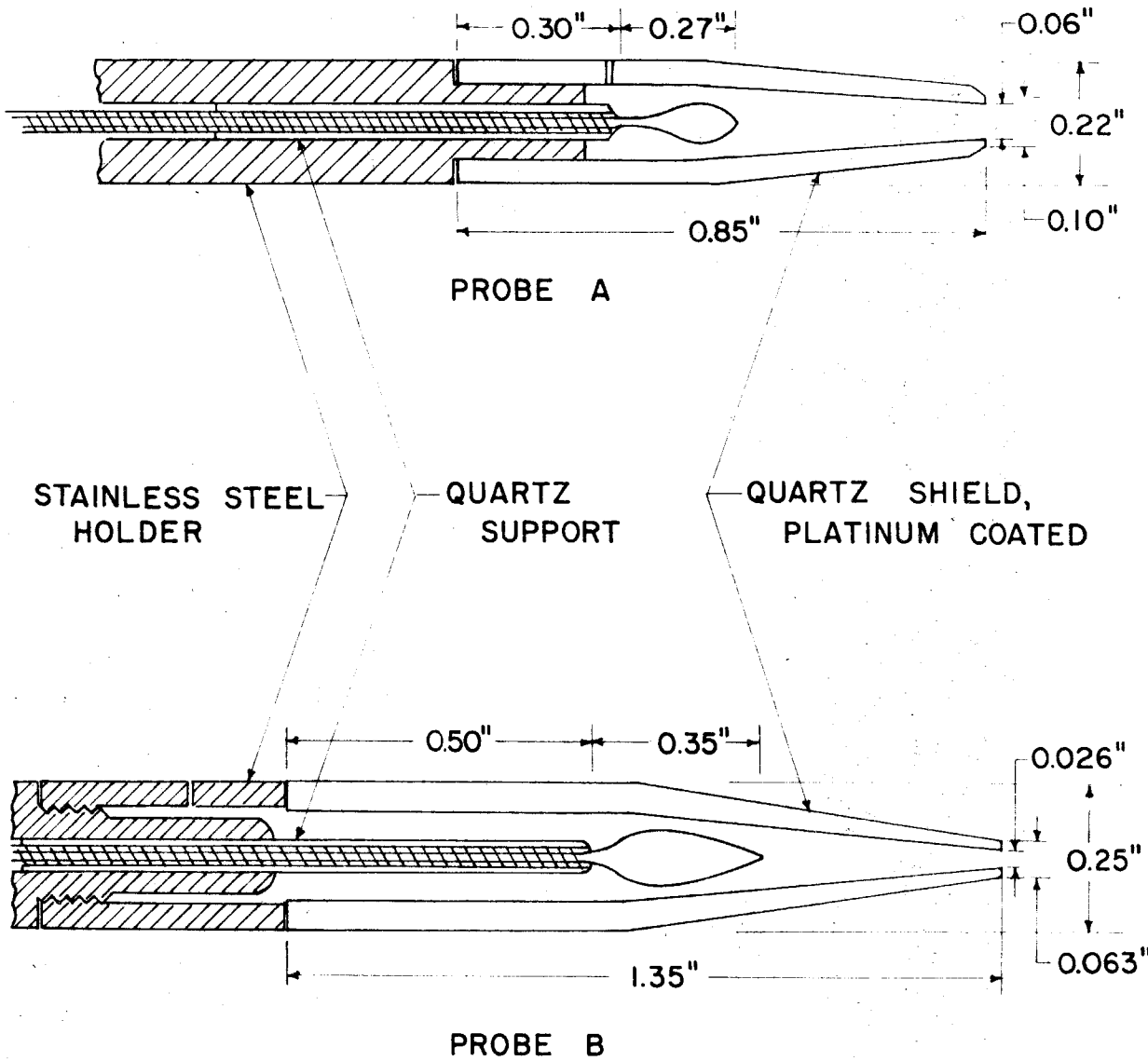

SKETCH OF STAGNATION-TEMPERATURE PROBES

FIG. 5

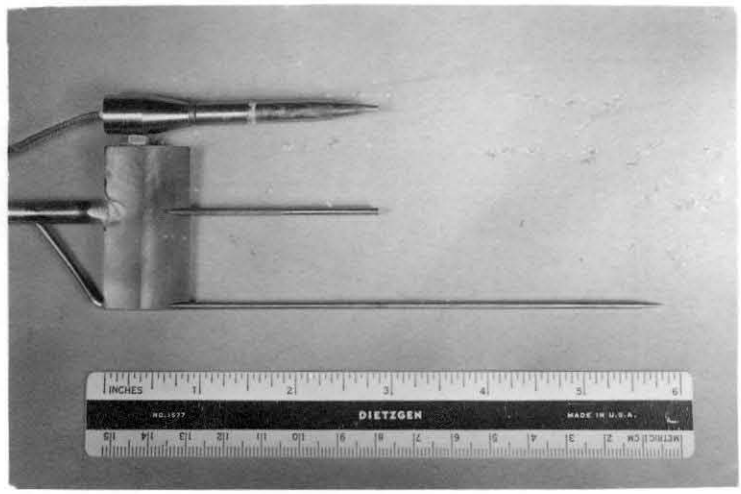

Fig. 6a

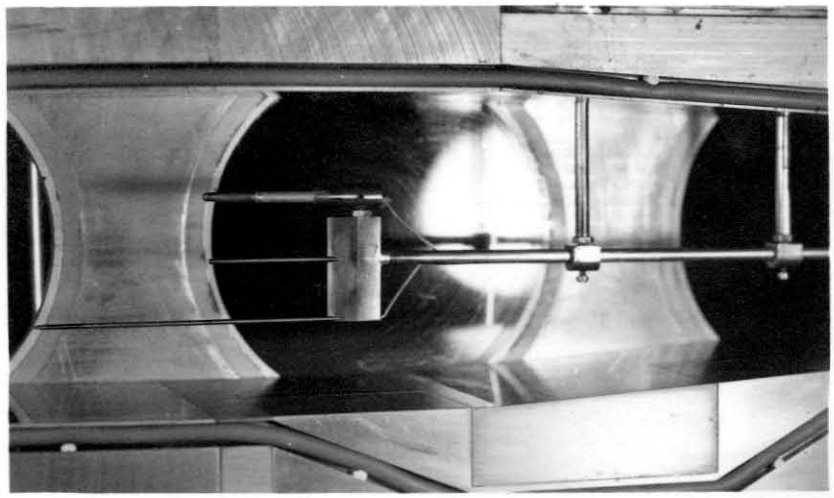

Fig. 6b

TEMPERATURE, IMPACT, AND STATIC-PRESSURE PROBE SUPPORT

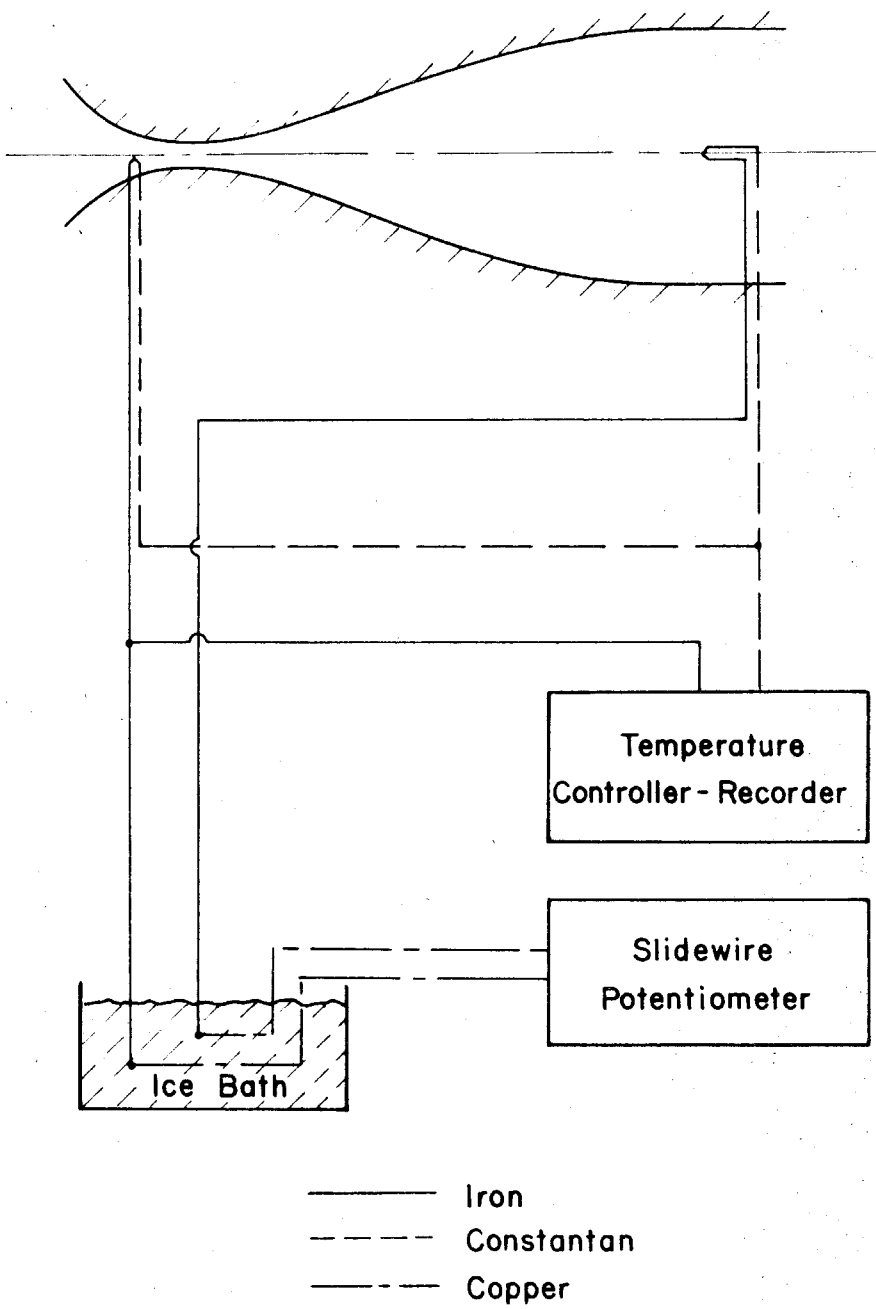

SCHEMATIC DIAGRAM OF ELECTRICAL CONNECTION FOR THERMOCOUPLE-POTENTIOMETER SYSTEM

FIG. 7

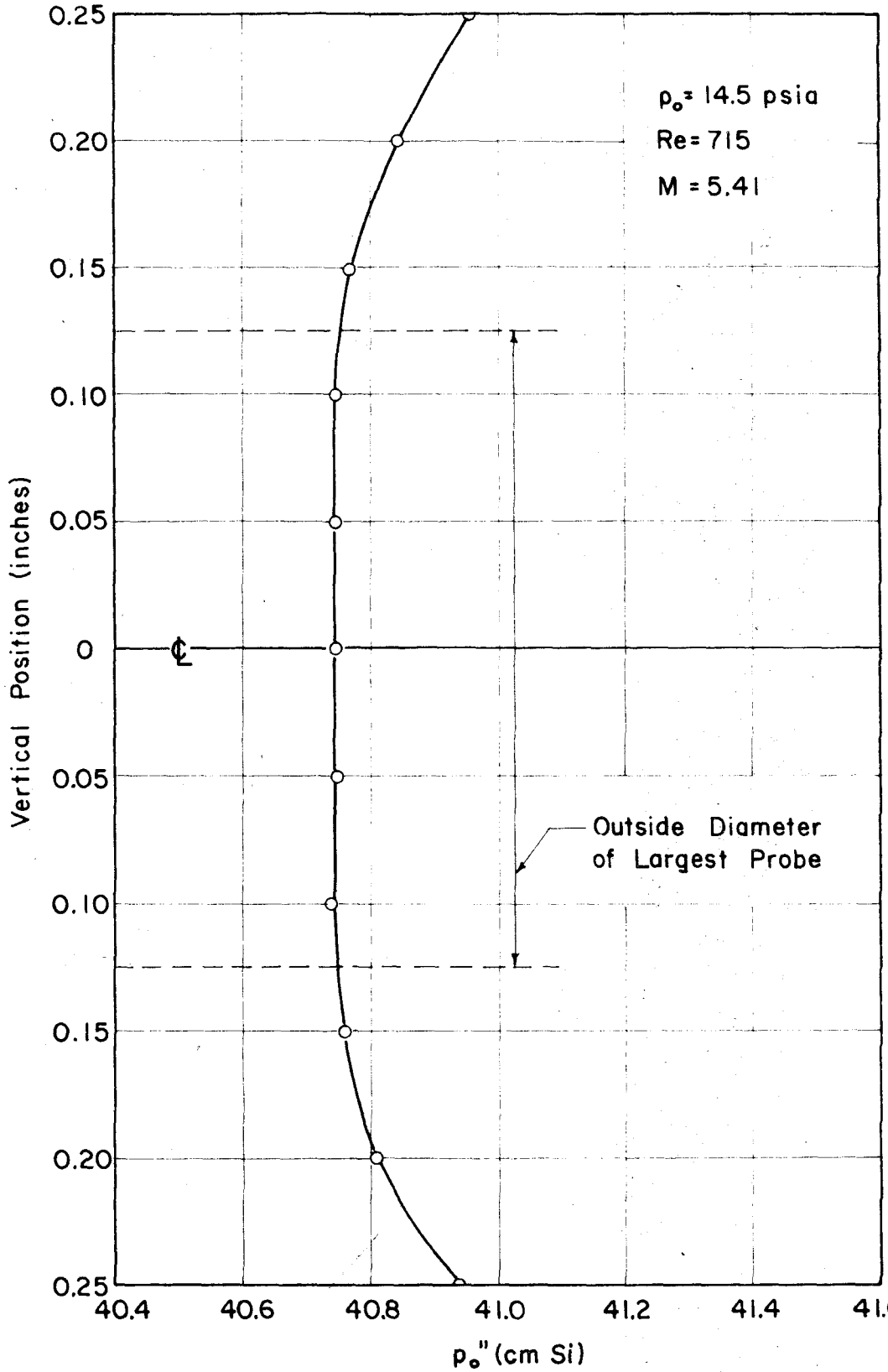

VERTICAL TOTAL-HEAD SURVEY IN LEG NO. 1

FIG. 8

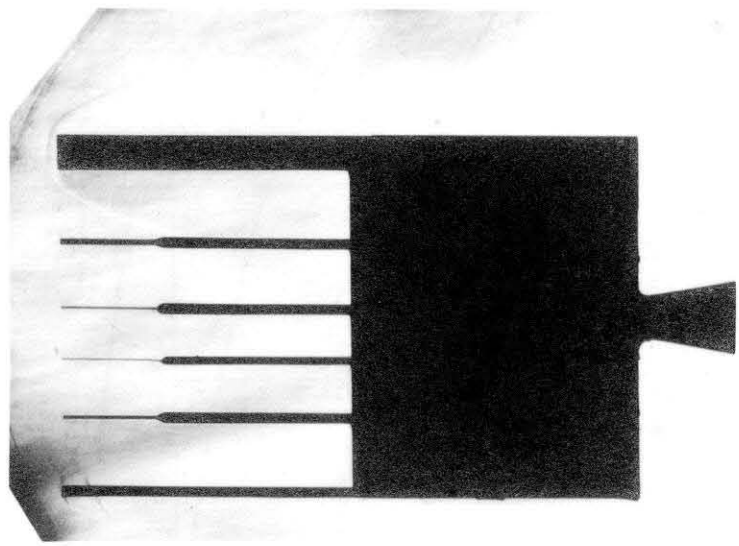

SCHLIEREN PICTURE OF AIR FLOW AROUND PROBE RAKE

Fig. 9

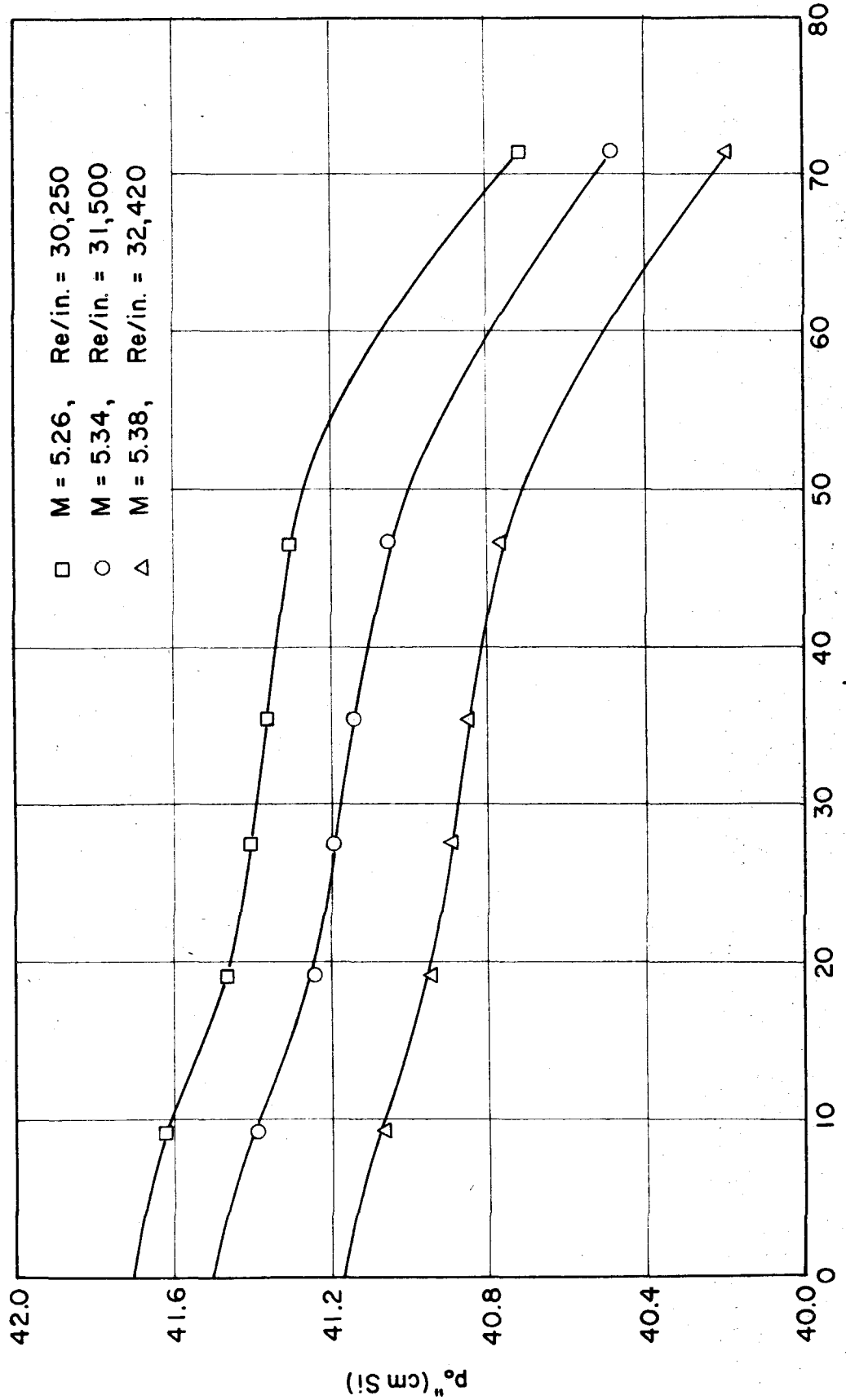

SAMPLE EXTRAPOLATION PLOTS OF IMPACT PRESSURE FOR TYPE II PROBES

FIG. 10

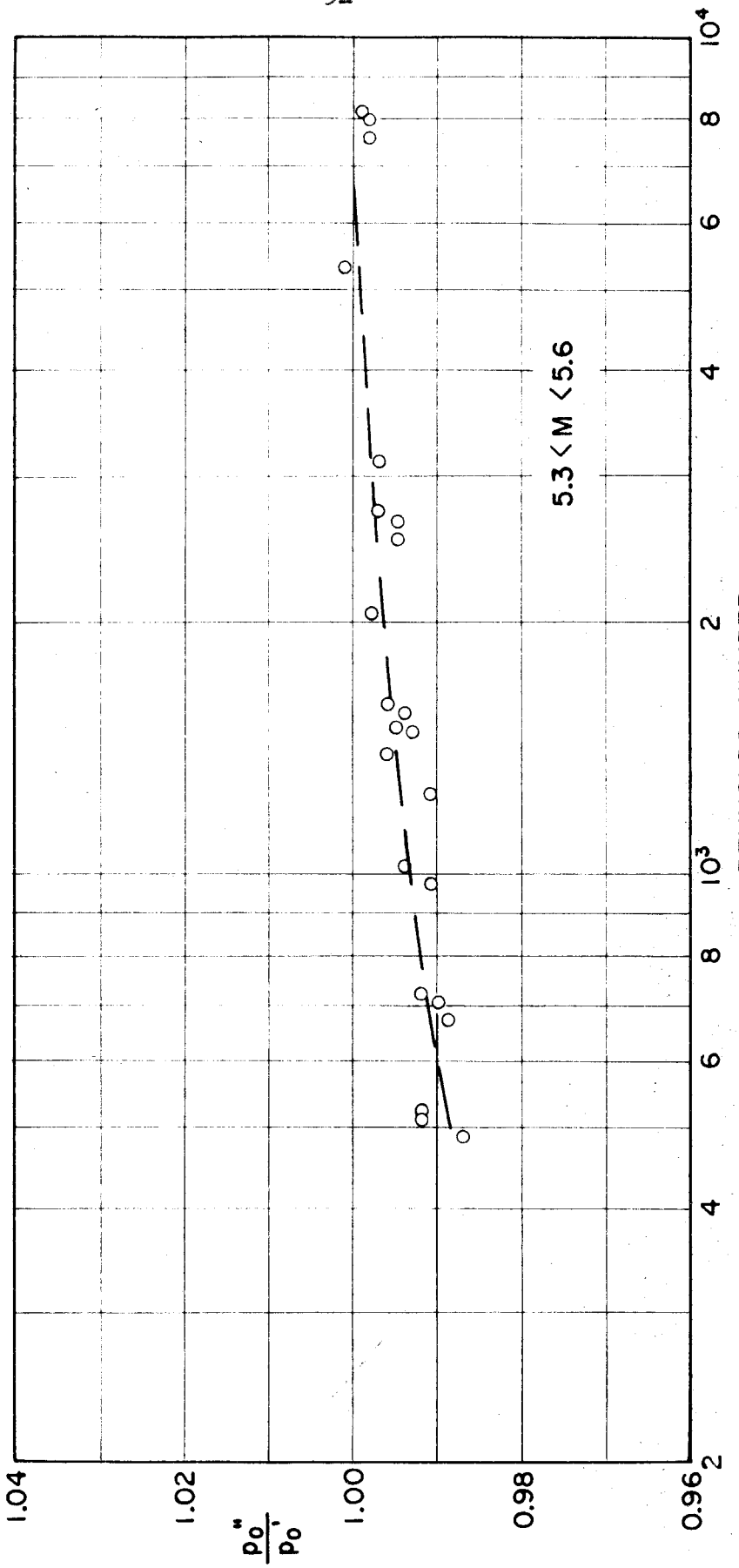

VARIATION OF MEASURED IMPACT PRESSURES WITH REYNOLDS NUMBER FOR TYPE I PROBES

FIG. 11

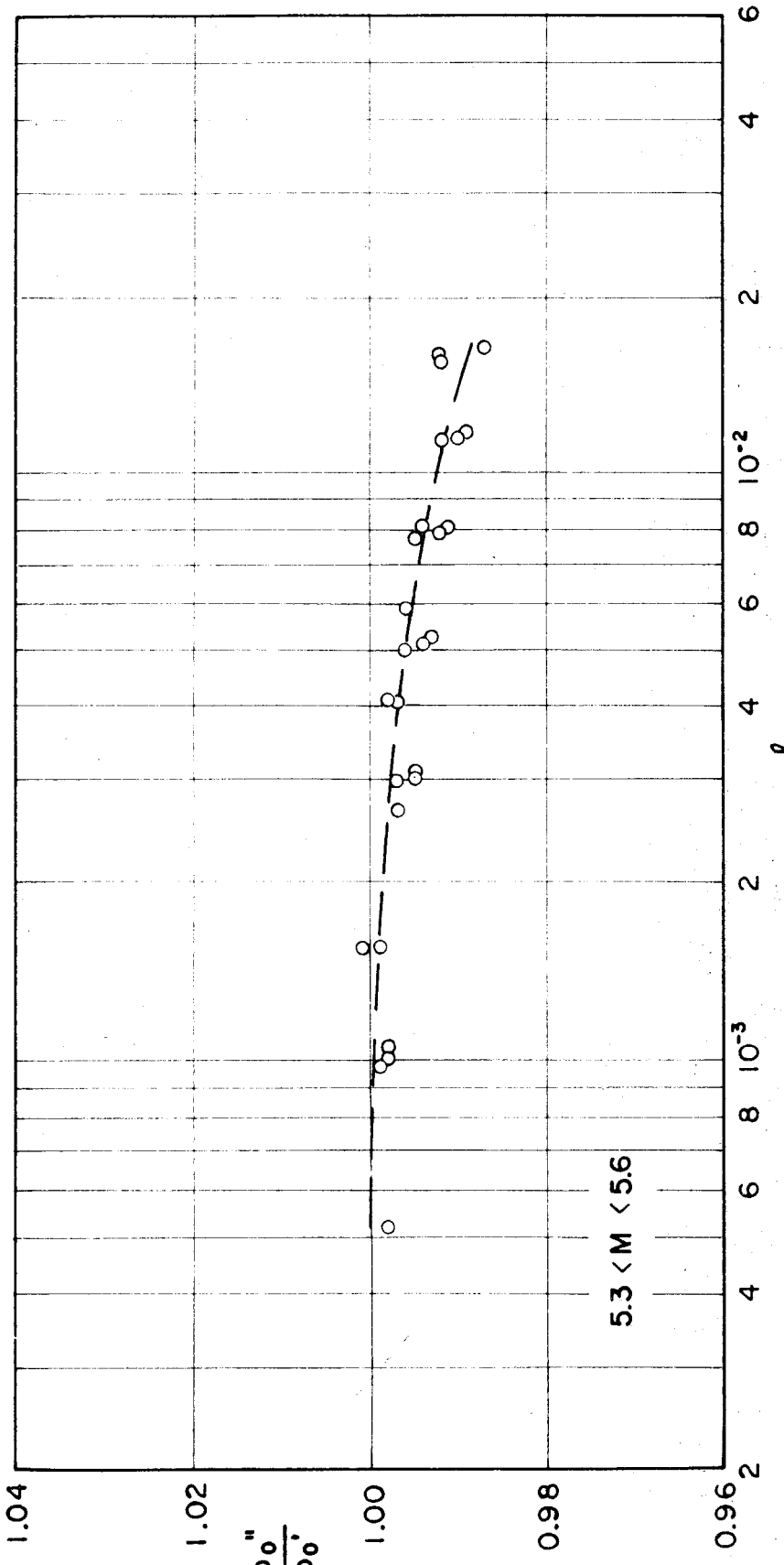

VARIATION OF MEASURED IMPACT PRESSURES WITH KNUDSEN NUMBER FOR TYPE I PROBES

FIG. 12

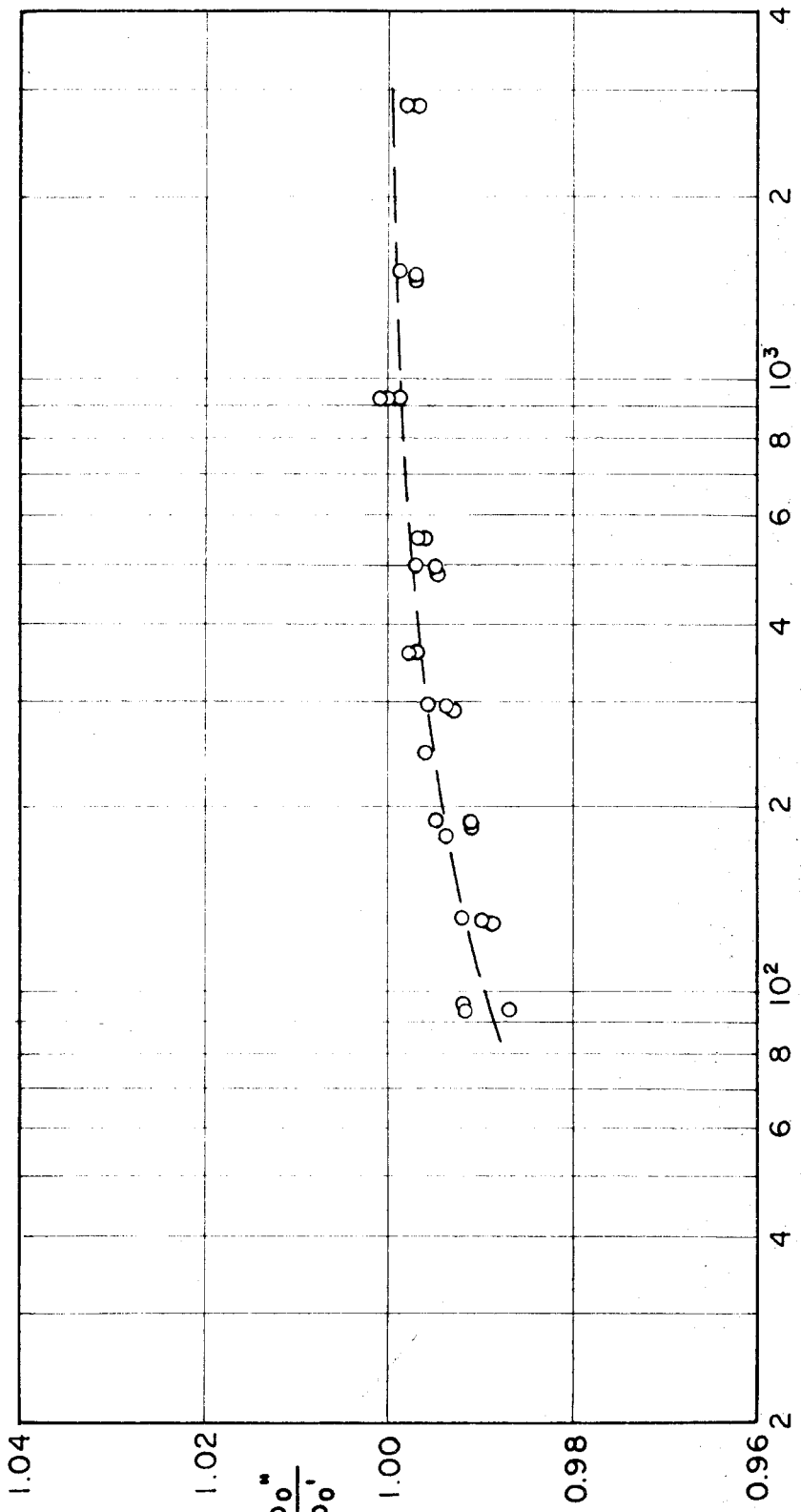

VARIATION OF MEASURED IMPACT PRESSURES WITH REYNOLDS NUMBER BEHIND NORMAL SHOCK FOR TYPE I PROBES

FIG. 13

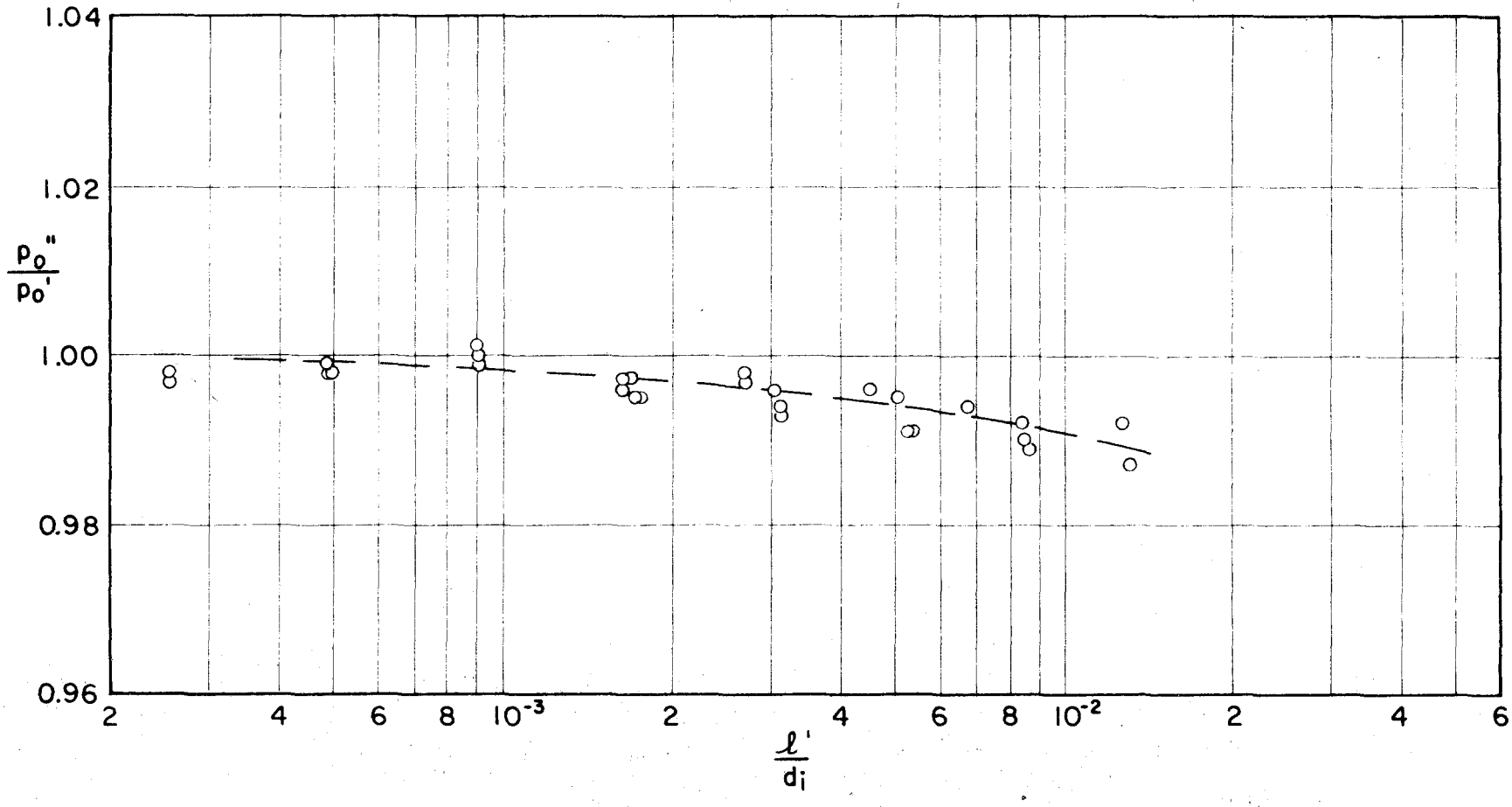

VARIATION OF MEASURED IMPACT PRESSURES WITH KNUDSEN NUMBER BEHIND NORMAL SHOCK FOR TYPE I PROBES

FIG. 14

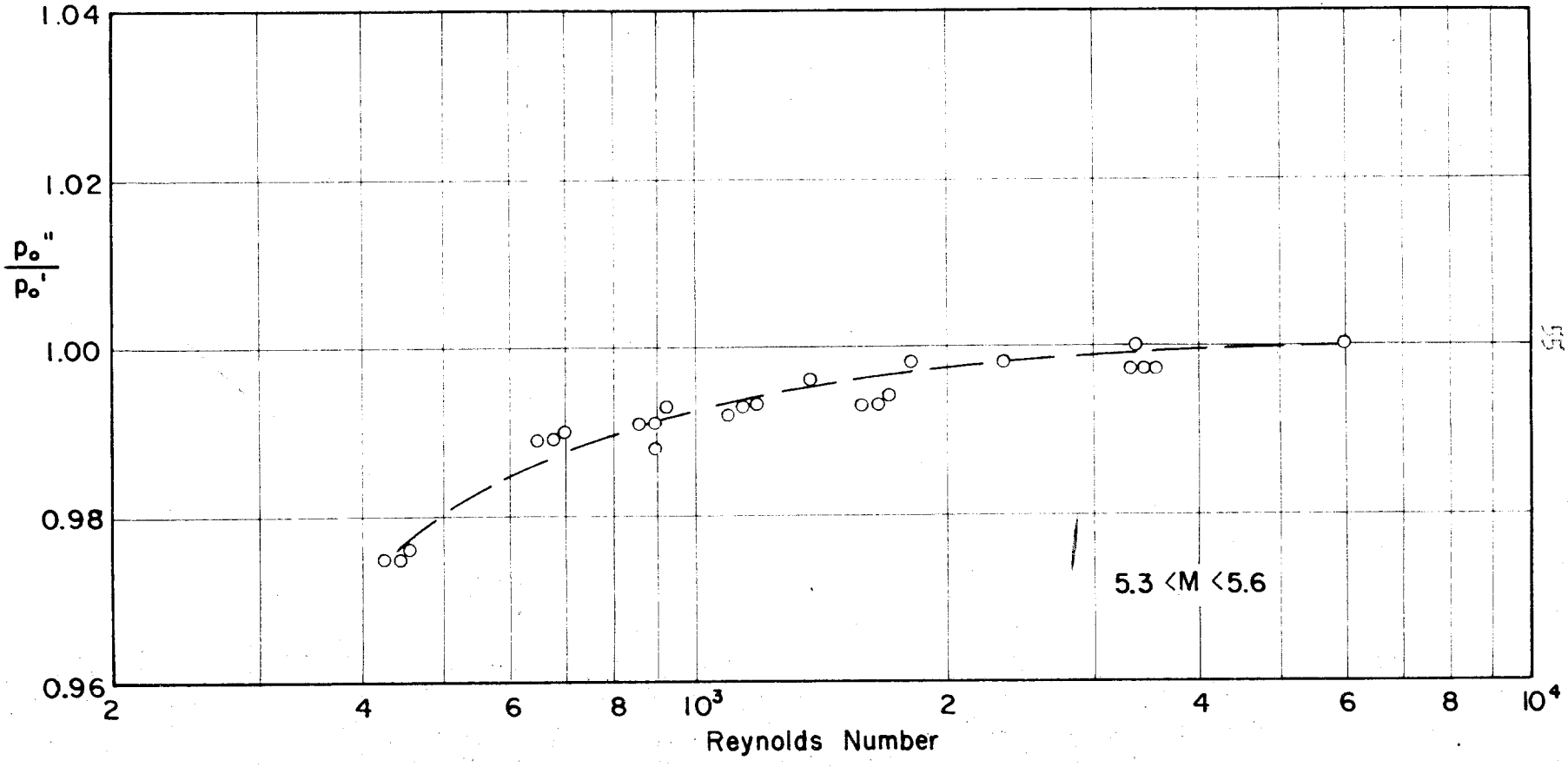

VARIATION OF MEASURED IMPACT PRESSURES WITH REYNOLDS NUMBER FOR TYPE II PROBES

FIG. 15

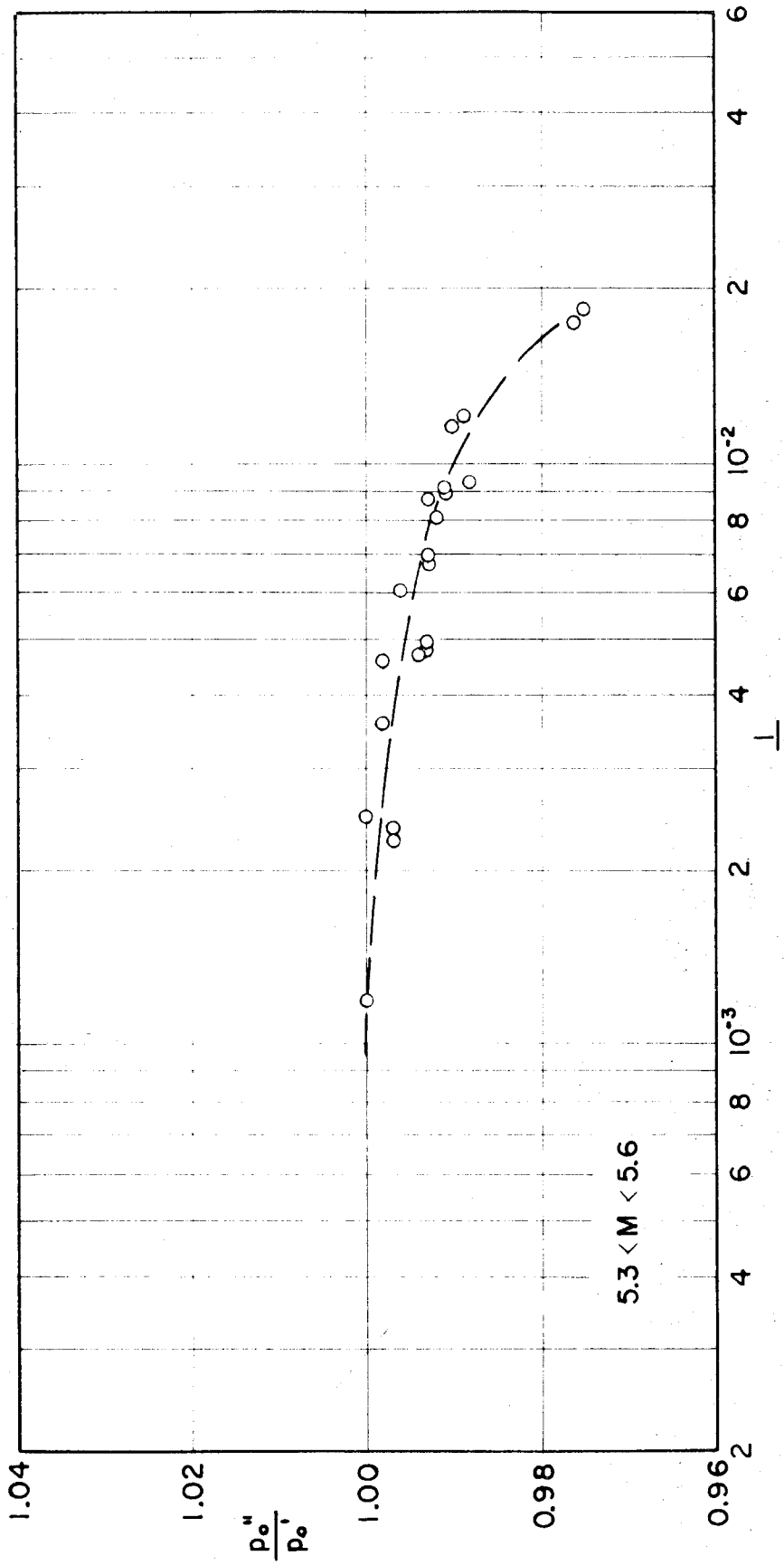

VARIATION OF MEASURED IMPACT PRESSURES WITH KNUDSEN NUMBER FOR TYPE II PROBES

FIG. 16

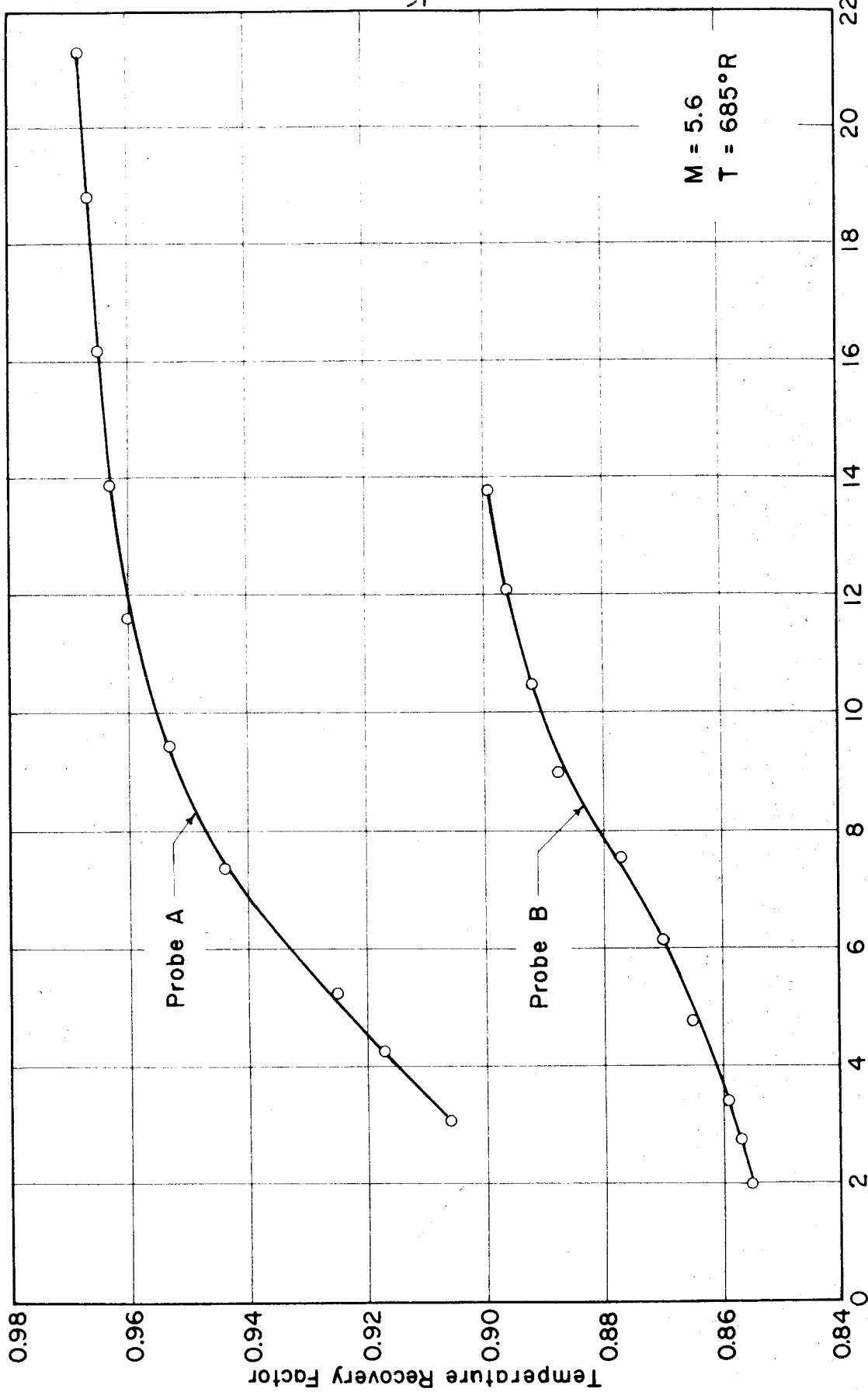

COMPARATIVE RECOVERY FACTORS FOR TWO TEMPERATURE PROBES

FIG. 17

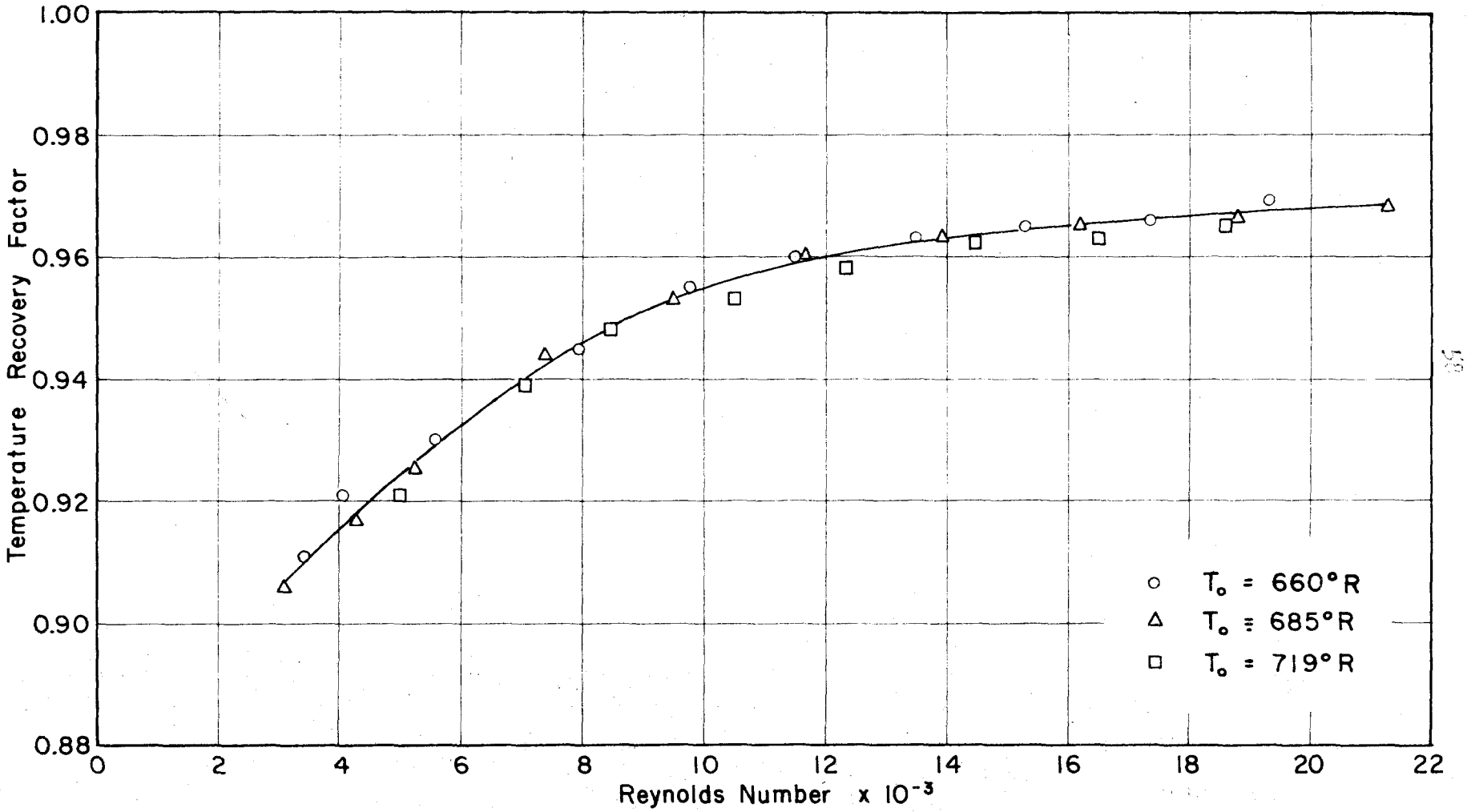

VARIATION OF RECOVERY FACTOR WITH REYNOLDS NUMBER FOR PROBE A

FIG. 18

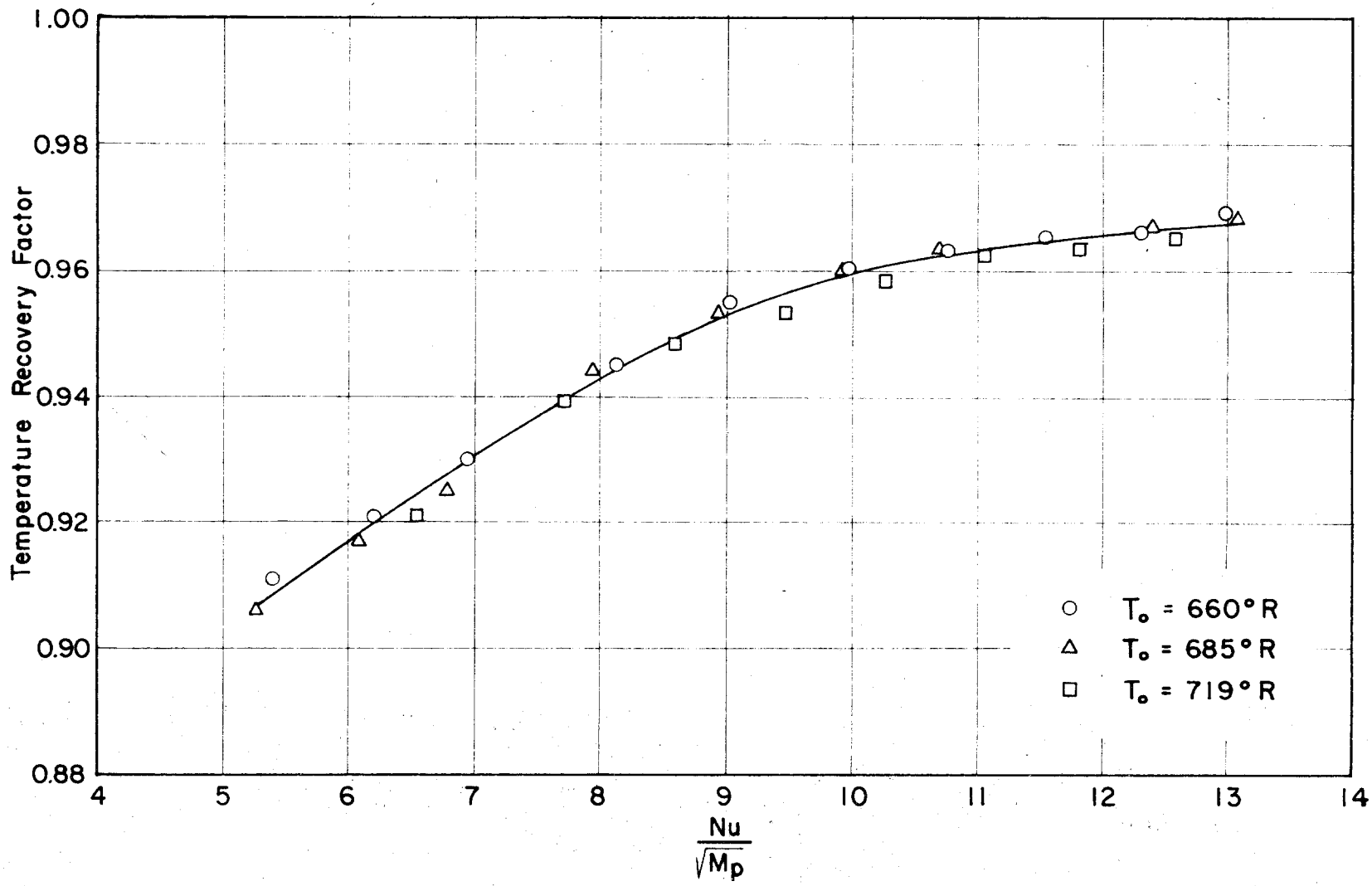

VARIATION OF RECOVERY FACTOR WITH NUSSELT NUMBER FOR PROBE A

FIG. 19

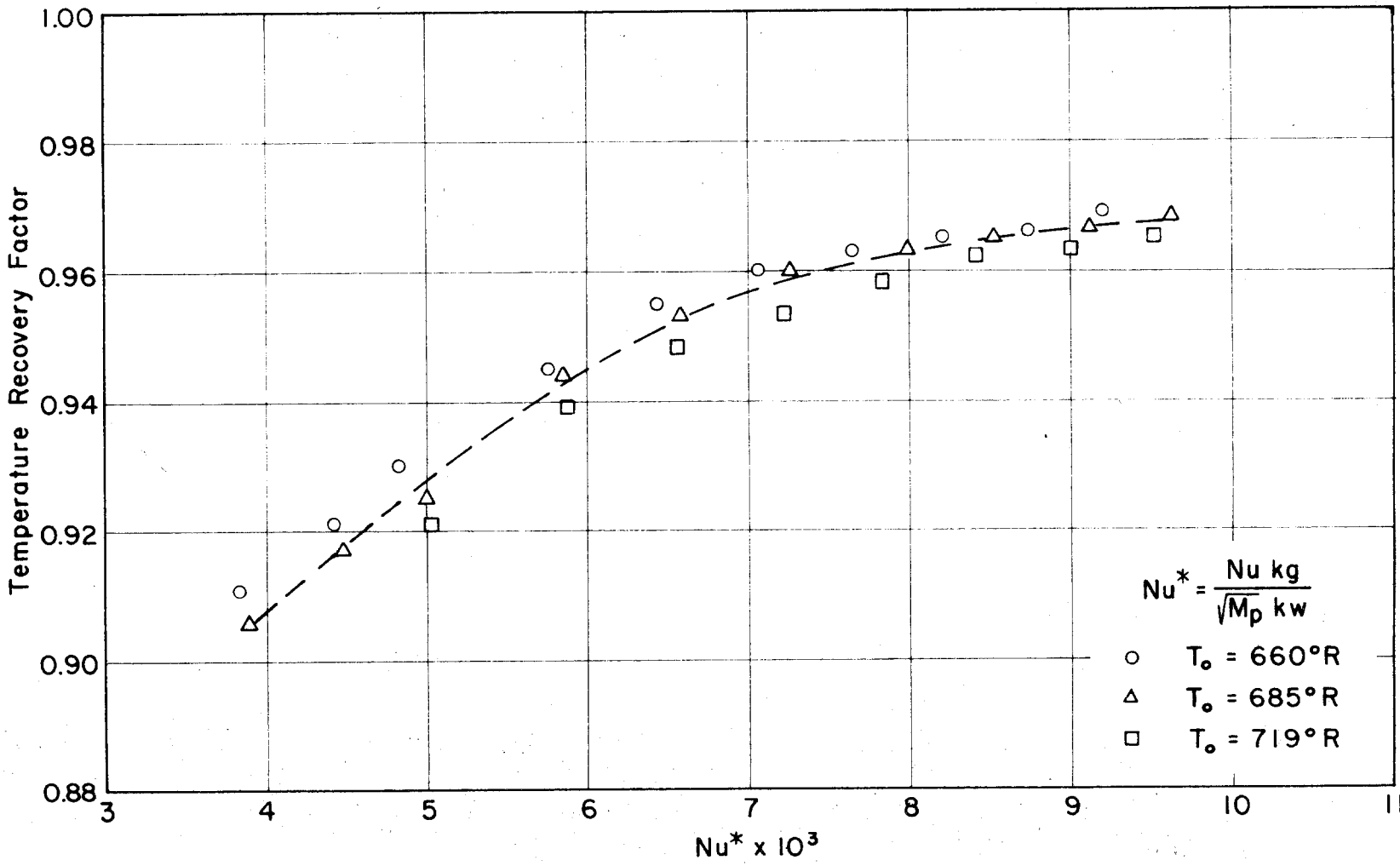

VARIATION OF RECOVERY FACTOR WITH Nu* FOR PROBE A

FIG. 20